Surface Ozone Distribution & Trends Over Ireland: Insights from long-term measurement record and source attribution modelling

Nikhil Korhale [1], Tabish Ansari [2], Tim Butler [2], Jurgita Ovadnevaite[1], Emmanuel Chevassus[1], Darius Ceburnis[1], Damien Martin[1,] Colin D.O'Dowd[1] , Liz Coleman[1]

1 School of Natural Sciences, Physics, Ryan Institute's Centre for Climate & Air Pollution Studies, University of Galway, Galway, Ireland

2 Research Institute for Sustainability (RIFS) at GFZ Helmholtz Centre for Geosciences, Potsdam, 14467, Germany

Corresponding author :

Name - Dr. Liz Coleman

Email Id – liz.coleman@universityofgalway.ie

Abstract

We present an analysis of long-term trends in surface ozone (O_3) across Ireland, with specific focus on the Mace Head atmospheric research station, representative of Northern hemispheric background atmospheric conditions. Surface O_3 dataset was characterised using advanced

trajectory analysis and seasonal decomposition, revealing distinct seasonal and spatial patterns. Findings show a significant rising trend in surface O_3 at Irish urban sites over the past two decades but without a similar trend at coastal sites. Highest O_3 levels and exceedances were observed at remote coastal sites, which are less susceptible to influence from local and easterly emissions but heavily influenced by transboundary pollution and stratospheric intrusion.

At Mace Head, springtime O_3 levels exhibit a declining trend, whereas wintertime levels show a rising trend. Focussing on the clean sector, the springtime decline remains significant, but without corresponding clean sector rising wintertime trends, implying the rising winter trends occur in response to declining local, United Kingdom (UK) and European emissions. Advanced modelling tools are used to quantify O_3 source contributions, elucidating key drivers behind the observed changes. Characteristic springtime O_3 maxima at Mace Head are predominantly attributed to stratospheric transport, hemispheric and long-range transport and lightning NO_x. The complementary trend and sectoral observational analysis reveal a decline in total spring-time concentrations, with a more rapid decline in exceedances from the UK & continental sector.

This research highlights the importance of seasonal factors in air quality management across Ireland, emphasising the need for a multi-faceted approach to control O_3 levels and reduce exceedances through global and regional emission reductions.

Keywords – Surface ozone, Meteorology, NO_x, Climate, CH_4, Emissions, VOC.

1. Introduction

Surface Ozone (O_3) has significant implications for health, vegetation, and climate. Its chemical production is driven by complex photochemical processes, responding non-linearly to pollution control, creating challenges for its effective regulation. Elevated O_3 levels cause severe health issues with prolonged exposure to high O_3 levels, causing respiratory issues,

cardiovascular problems, and reduced lung function, particularly in sensitive populations such as children, the elderly, and individuals with pre-existing respiratory conditions (Lin et al., 2018; Todorović et al., 2019; Zhang et al., 2019, WHO, 2021). O_3 pollution can adversely impact vegetation by reducing agricultural productivity (Ashmore et al., 2005; Paoletti et al., 2006). O_3 is also the third most significant greenhouse gas after Carbon Dioxide (CO_2) and methane (CH_4), contributing to climate instability (IPCC, 2021). O_3 can live for several weeks in the free troposphere, and it is affected by large-scale atmospheric circulation patterns (Wespes et al., 2017). Meteorological factors such as temperature, solar radiation, wind speed, and atmospheric stability play a significant role in O_3 formation. (Ding et al., 2023; Khiem et al., 2010).

O_3 is formed in the atmosphere from precursors Nitrogen Oxides (NO_x), carbon monoxide (CO), and volatile organic compounds (VOCs) through photochemical reactions. Photochemical production requires solar radiation, and reaction rates are correlated with temperature, it is noted that little photochemical production occurs at temperatures below 20^{o}C (Coates et al., 2016). The reactive, interdependent atmospheric chemistry leads to a non-linear relationship between O_3 and its precursors (Seinfeld and Pandis, 2016), and effective O_3 mitigation requires an understanding of processes influencing O_3 production and removal mechanisms (Fowler et al., 2013).

NO_x can suppress or enhance O_3 formation, depending on local atmospheric chemistry regime. In polluted urban environments, high NO_x emissions can lead to O_3 dissociation, retarding photochemical O_3 formation (NO_x-saturated/VOC-limited regime), with local pollution events potentially titrating surface O_3 completely, converting NO to NO_2. This effect is more prevalent in wintertime, when temperatures are low, and there is little solar radiation to facilitate photochemical production of O_3. In relatively clean environments, O_3 formation is correlated with NO_x concentration (Tavella & da Silva Júnior, 2021).

O_3 and precursors can be transported over great distances in the troposphere, with transport from distant polluted regions accounting for 40% of O_3 abundance in remote regions (Sudo and Akimoto, 2007). While O_3 is transported in air masses from distant sources, although titration occurs, O_3 is replenished via mixing. Over Ireland, advection of O_3 rich air from continental outflow is a significant source of Irish O_3, but European continental air-masses can also transport pollutants to trigger O_3 depletion events, but the O_3 depleting effect of the air masses originating from Europe is in decline in response to European Union (EU) pollution control strategies (Derwent et al., 2024).

Seasonal and regional variations further complicate the regulation, with higher O_3 levels observed in summer across the northern hemisphere due to increased temperatures, solar radiation, and abundant precursors (Moiseenko et al., 2021; Sicard et al., 2016). In marine boundary layers, O_3 levels are generally lower than in continental regions, though specific oceanic environments can exhibit high O_3 concentrations due to inflows from polluted areas (Boylan et al., 2014; Girach et al., 2020). Another factor which influences O_3 levels is the North Atlantic Oscillation (NAO), which influences O_3 levels in Western Europe. During a positive NAO phase, O_3 levels increase. In contrast, during a negative NAO phase (NAO-low), O_3 levels decrease. This effect is particularly notable in southwest, central, and northern Europe (Bonaccorso et al., 2015; Creilson et al., 2003; Pausata et al., 2012).

While Ireland's air quality is mostly governed by the influx of clean maritime air from the Atlantic Ocean (Tripathi et al., 2010), certain synoptic scenarios allow for the intrusion of polluted air masses from continental Europe. These events, though infrequent, can bring substantial amounts of O_3 and its precursors (NO_x and VOCs), contributing to short-term O_3 pollution episodes.

The World Health Organisation (WHO) publishes Air Quality Guidelines (AQGs) as a non-legally binding global target for governments to achieve within their jurisdictions. These

AQGs comprise evidence-based recommendations of limit values to protect public health. The current recommended AQGs for O_3 is expressed as a daily maximum of 8-hourly running average O_3 value of 100 μg/m³. Days when O_3 levels exceed the recommended AQGs are classified as exceedance days. Factors contributing to exceedances include high solar radiation, stagnant air masses, and local emissions and regional and transboundary transport of O_3 and precursors. Globally, over the past 150 years, there has been a 40% increase in O_3 levels owing to rising precursor emissions. (Archibald et al., 2020; Griffiths et al., 2021; Young et al., 2013). Despite European Union emission reduction policies, O_3 pollution remains a problem, with over 94% of those living in European cities exposed to O_3 levels exceeding the WHO AQGs in 2022 (EEA 2024, WHO 2021). Over 22,000 premature deaths in the EU were attributable to short-term exposure to O_3 in 2021 (Soares et al., 2023).

Long-term O_3 measurement data from the Mace Head research station in Ireland reveal a distinct seasonal pattern with peaks during spring and lows in summer. (Derwent, 1998; Derwent et al., 1994, 2018). Historical trends show increasing baseline O_3 levels in the 1980s and 1990s, stability in the 2000s, and a decline in the 2010s (Derwent et al., 2013; Derwent et al., 2018). Recent observational and modelling data have identified a broad O_3 maximum in spring and early summer, aligning with peak stratospheric transport (Ansari et al., 2024; Lin et al., 2012; Russo et al., 2023). O_3 dynamics are complex, and studies reveal discrepancies between model output and observations (Bessagnet et al., 2016; Vautard et al., 2012), highlighting the need for further understanding of factors governing O_3 levels and trends.

This study investigates the distribution and trends of O_3 and its precursors across Ireland, providing valuable insights into the regional and hemispheric impact on Irish surface O_3 levels and exceedances. We analyse the long-term O_3 observational dataset for Ireland, identifying the mean and range of O_3 levels and seasonal variation at each site. We identify the long-term

annual and monthly trends at each site, quantifying the significance of each trend according to TOAR guidelines (Chang et al., 2023). We also identify the frequency and seasonality of exceedance of the WHO AQGs for the protection of human health from O_3 pollution for each site. The trends and seasonality are contextualised by looking at trends in the Irish instrumental record of dominant precursors of NO_x and CH_4 and we discuss the relationship between NO_x and O_3 by comparing anomalies between monthly average NO_x and O_3 during lockdown compared to the average values for the three years prior to lockdown. Advanced modelling results using the Tropospheric Ozone Attribution of Sources with Tagging 1.0 (TOAST 1.0) framework (Butler et al., 2018; Butler et al., 2020) are validated against measurements at various sites for simulation period 2000-2018, and the simulation results analysed to determine the geographical and sectoral source of precursors that contribute to simulated O_3 at Mace Head, identifying seasonality and long-term trends in the sources. Finally, the observational data are classified using advanced trajectory clustering methods to separate air masses from the clean sector from those influenced by local, UK or EU emission sources, with seasonal trends identified for both clean and polluted sectors, and the exceedances classified as coming from either the clean or polluted sector.

This research highlights significant seasonal and temporal variations and long-term trends in O_3 concentrations, and the integrated approach, including observational and modelling analysis, enhances our understanding of the drivers of O_3 concentrations, trends and exceedances over Ireland and allows quantification of global and regional contributions to Irish surface O_3.

2. Data and methodology

2.1 Observational Network and Analysis Approach

Measurement data is obtained from the Environmental Protection Agency, Ireland (EPA) (https://eparesearch.epa.ie/safer/). The O_3 monitoring network shown in Figure 1 has been operational in Ireland since 1994. O_3 is measured using an API M400 and O_3 analyser based on UV photometry at all monitoring sites. At the Mace Head site, O_3 was measured using a Monitor Labs 8810 analyzer and a Thermo Environmental O_3 monitor. Measurement operating accuracy is within 1.0 ppb, based on precision, calibration and drift characteristics. Measurements of O_3 precursors from EPA air quality monitoring sites are also monitored. The details of the measurements sites are shown in Table 1. Numerous previous studies have analysed this data, with a particular focus on the analysis of Mace Head data to assess background O_3 (Carslaw, 2005; Derwent et al.,1994, 1998, 2001, 2004, 2008, 2013; Derwent, Manning, Simmonds, & Doherty, 2018; Derwent, Manning, Simmonds, Spain, et al., 2018; Oltmans et al., 2013; Simmonds et al., 2004; Tripathi et al., 2010, 2012, 2013). CH_4 data is obtained from the Integrated Carbon Observation System (ICOS) network, accessible at https://www.icoscp.eu/data-products/ATM_NRT_CO2_CH4.

For this analysis, the observational sites were classified into three categories: Coastal, Rural, and Urban, as shown in Figure 1. The classification of the sites is based on Spohn et al., 2022, with the addition of the coastal category. Hourly data were used to evaluate annual trends based on monthly mean concentrations. Seasonal analysis conducted for the four main meteorological seasons in Ireland, namely Spring (March, April, May), Summer (June, July, August), Autumn (September, October, November), and Winter (December, January, February). O_3 exceedances were calculated based on the WHO AQGs, indicating that the maximum daily average over eight hours (MDA8) should not exceed 100 $\mu g/m^3$. A significant analysis was performed on data measured at the Mace Head Atmospheric

167 Research Station (53°33′N, 9°54′ W), which is exposed to pristine marine air masses
168 approximately half of the time. (Grigas et al., 2017; O'Dowd et al., 2014).

169 **Table 1.** Details of Environmental Protection Agency Ireland (EPA) O_3 measurement sites
170 over Ireland, with location information, and the data period used for the study.

171

Site	Data availability	Type	Latitude	Longitude
Mace head	1994-2022	Coastal	53.3253	-9.9036
Valentia	2001-2022	Coastal	51.9385	-10.24
Monaghan	1995-2022	Rural	54.0661	-6.883
Laois	2005-2022	Rural	53.1076	-7.1983
Kilkenny	2012-2022	Rural	52.6383	-7.2676
Castlebar	2009-2022	Rural	53.851	-9.3003
Rathmines	2002-2022	Urban	53.322	-6.2672
Clonskeagh	2008-2022	Urban	53.3118	-6.2353
Swords	2009-2022	Urban	53.4631	-6.2222
Wicklow Bray	2009-2022	Urban	53.1873	-6.122
Cork South link road	2014-2022	Urban	51.8785	-8.4649
Cork Bishops town	2016-2022	Urban	51.8858	-8.53321
Cork UCC	2018-2022	Urban	51.9	-8.4863

172

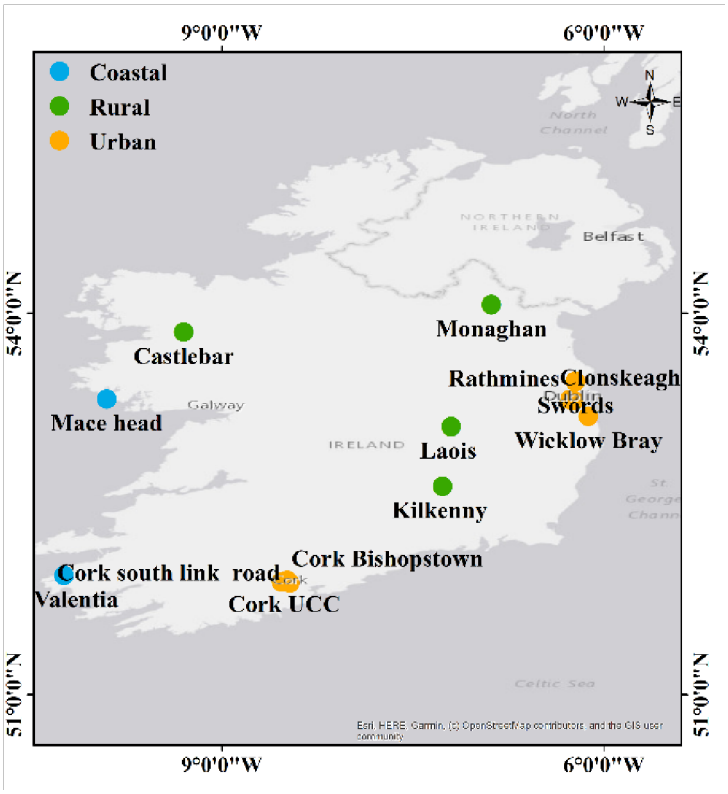

Figure 1. – The map of EPA O_3 measurement sites over Ireland with classification of backgrounds.

Trend analysis was conducted using the Openair package in R, software designed for the analysis of atmospheric composition data. Trends were determined using the Theil-Sen slope estimator and Mann-Kendall tests to quantify significance, in accordance with the Tropospheric Ozone Assessment Report (TOAR) guidelines (Lefohn et al., 2018). Theil-Sen directly provides a robust slope estimate. It is a reliable measure of change over time for direct interpretation and comparison. It is a robust method for estimating trend slopes in time series data, preferable to traditional least-squares regression, which can be sensitive to extreme values and outliers. Uncertainty or reliability of the trend is calibrated according to the p-value, as outlined by (Chang et al., 2023), consistent with the best statistical practices for analysis used in the second phase of TOAR.

2.2 Clean air sector identification from Back trajectories

Baseline O_3 refers to the concentration of O_3 in air masses minimally influenced by local or regional anthropogenic emissions. Back-trajectory methods are widely used to estimate baseline O_3 levels by analysing the origins and transport pathways of air masses reaching observation sites. Typically, Lagrangian dispersion models are used to trace air parcels backwards in time and identify their origin.

For this study, air mass trajectories arriving at Mace Head were calculated using the Hybrid Single Particle Lagrangian Integrated Trajectory Model (HYSPLIT) (Draxler et al.,2003; Stein et al., 2015) in conjunction with R software. The air masses were classified into two categories: the clean sector and EU-influenced sector. An air mass was considered part of the clean sector when air mass trajectories remained over the ocean surface for the previous 72 hours, the remaining air mass trajectories are classified as the EU-influenced sector. Meteorological data for the analysis were derived from NOAA reanalysis data (Stunder et al., 2004). The 72h duration captures regional/long-range transport without trajectory error from meteorological uncertainties. The 100 m height was used to represent the well-mixed flow of the boundary layer above the surface. The 06:00 UTC aligns with synoptic times and can match daily O_3 cycles or measurement periods. Therefore, calculations were performed for 6:00 UTC each day, with a final trajectory height of 100 meters, covering the years 2000 to 2022. The O_3 concentrations observed during the clean sector were averaged to derive baseline levels, consistent with previous studies on baseline O_3 trends and sources (Derwent et al., 2013; Oltmans et al., 2006).

2.3 CAM4-Chem Model

The CAM-Chem air quality model, part of the Community Earth System Model (CESM), simulates atmospheric chemistry and the interactions among chemical constituents, meteorology, and climate. It incorporates detailed chemical mechanisms, emission inventories,

and meteorological data to simulate pollutant dispersion, thereby allowing us to determine air quality trends. CAM-Chem has been applied in numerous studies, significantly contributing to the understanding of regional and global atmospheric processes. (Lamarque et al., 2012; Tilmes et al., 2016). The model features a flexible chemical pre-processor to allow for detailed handling of atmospheric chemistry. Studies have demonstrated that CAM-Chem accurately represents conditions in both the troposphere. (Aghedo et al., 2011; Lamarque et al., 2010) and the stratosphere (Lamarque et al., 2008; Lamarque and Solomon, 2010), including temperature structure and dynamics (Butchart et al., 2011). Offline CAM-Chem has also been utilised in the Hemispheric Transport of Air Pollution (HTAP) assessments. (Anenberg et al., 2009; Fiore et al., 2009; Jonson et al., 2010; Shindell et al., 2008; Tan et al., 2018).

For the current study, we analyse simulations of the Community Atmospheric Model version 4 CAM4-Chem (Community Atmosphere Model version 4 with chemistry) (Lamarque et al., 2012). The model simulations were carried out at a horizontal resolution of 210 km × 280 km, with 56 vertical levels for the 2000-2018 period, with specified dynamics derived from MERRA2 reanalysis. (Molod et al., 2015). The coarse spatial resolution, it is still appropriate because it provides a reliable representation of the regional background atmosphere influencing the urban sites. The model captures large-scale features of atmospheric transport, seasonal variability, and background O_3 levels, all of which are essential for interpreting urban observations. Comparing urban measurements with regional-scale CAM-Chem outputs allows local pollution effects to be distinguished from regional atmospheric influences.

Tagged source attribution of tropospheric ozone (TOAST 1.0) is a novel tagging methodology developed for the CESM to quantify source contributions to O_3. Unlike traditional methods that rely on sensitivity simulations, TOAST uses an online tagging approach to track O_3 production from specific NO_x and VOC sources (e.g., anthropogenic, biogenic, biomass burning, lightning) directly within the model, allowing for efficient attribution of O_3 to regional

and sectoral emissions while maintaining full chemical coupling. The tool has been validated against observations and demonstrates utility in disentangling the impacts of different emission sectors on O_3 pollution. (Butler et al., 2018, 2020; Lupaşcu et al., 2022; Nalam et al., 2025).

The model results have inherent standard uncertainties common in any modelling exercise, i.e., uncertainties in emission inventories in terms of magnitude and spatial accuracy; uncertainties in model parameters, e.g., surface resistance for deposition for various surfaces, boundary layer mixing, photolysis, chemical kinetic parameters (Wild et al., 2025) and structural deficiencies such as a coarse resolution and missing processes (e.g., halogen chemistry; Saiz-Lopez et al., 2025). The sum of all tagged contributions very closely matches the total simulated ozone (which is simulated independently and is not just an algebraic sum of the tagged contributions) is a good validation of the tagging mechanism (Butler et al., 2018 and 2020).

Global CAM4-Chem model simulations are performed for the years 2000-2018 with NO_x and VOC tagging (as described in Ansari et al., 2025; Nalam et al., 2025), with the base chemical mechanism (Emmons et al., 2012) and source code modified to account for extra tagged species representing regional and sectoral identities. Anthropogenic emissions of NO_x, CO, and non-methane volatile organic compounds (NMVOCs) are incorporated from the Hemispheric Transport of Air Pollution version 3 emissions inventory. (HTAPv3; Crippa et al., 2024), which includes land-based emissions, international shipping emissions, and aircraft emissions. Biomass burning emissions are sourced from the GFED-v4 inventory (Van Der Werf et al., 2010), while biogenic NMVOC emissions are derived from CAM4-GLOB-BIOv3.0. The O_3 source attribution technique used for this study is described in (Butler et al., 2020).

3. Results and discussions

3.1 Yearly variation of O_3

Figure 2 shows box plots, illustrating the average O_3 concentrations for 13 sites over the duration of the available dataset, as discussed in section 2.1, providing a comprehensive overview of the variability and distribution of O_3 concentration. Coastal sites, Mace Head and Valentia, show higher O_3 levels compared to other sites, with annual average concentrations of 77 µg/m³ and 69 µg/m³, respectively. In urban areas like Rathmines, Dublin, O_3 concentrations remained consistently lower, with averages ranging from 39 to 56 µg/m³. Similarly, South link road and Bishopstown sites in Cork city, recorded relatively lower concentrations compared to coastal and rural locations, reflecting the impact of high urban NO_x emissions. Rural sites like Laois and Kilkenny showed intermediate O_3 concentrations, less influenced by urban emissions. These sites consistently show O_3 averages ranging between 50 to 57 µg/m³, with little variability, highlighting the predominant role of steady background O_3 contributions in rural sites. O_3 concentrations vary significantly with proximity to emission sources adjacent to urban areas. O_3 levels can be lower due to titration, where O_3 reacts with NO, causing O_3 depletion, but the transport of precursors can cause an increase in O_3 concentration downwind of the sources (Jeon et al., 2014; Monks et al., 2015; Zhu et al., 2012)

The red line over the box shows a clear seasonal pattern in O_3 concentration for each site, with a springtime (March-April) peak and summertime (June-July) dip, with the highest peaks in the coastal sites, and lowest dips in urban sites, influenced by local emissions, e.g. Cork South Link Road and Swords.

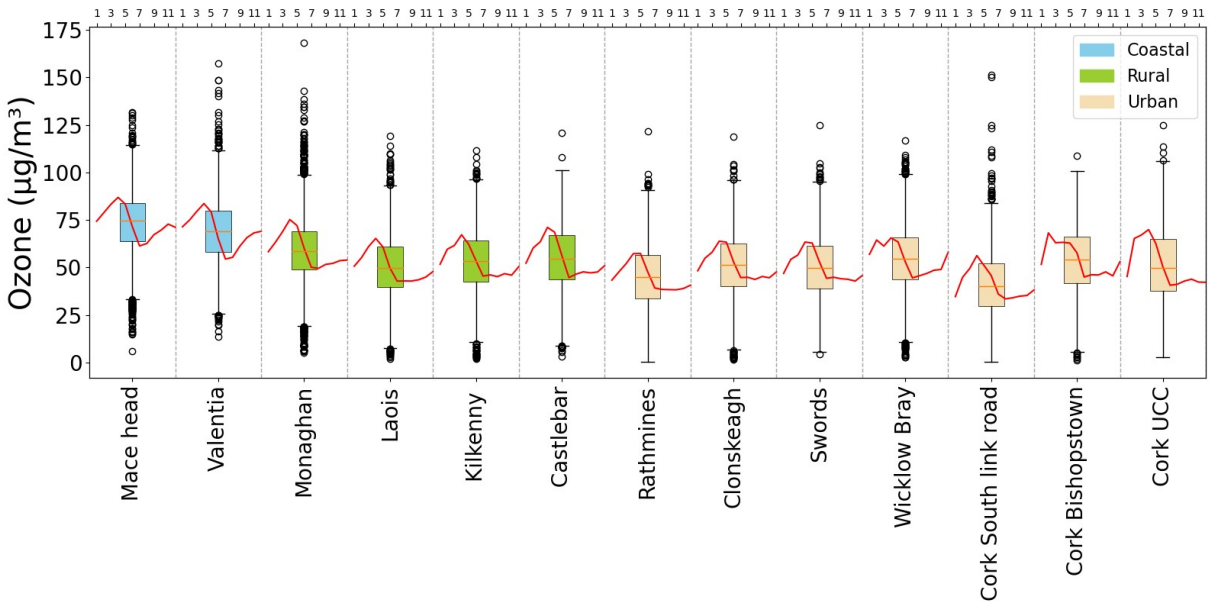

Figure 2. Annual average O_3 concentration at different sites in Ireland. In each box, the lowest whisker level represents the 5th percentile, the box spans from the 25th to the 75th percentile, the horizontal line within the box represents the median 50th percentile, and the upper whisker represents the 95th percentile. The average of monthly O_3 values calculated for the entire period of each station, and the red line shows the average monthly O_3 variation of all sites top axis shows the month (1– 12).

3.2 O_3 Trend analysis

3.2.1 Yearly trend

Table 2 summarises the Theil-Sen trends in O_3 concentration (in µg/m³ per year) across 13 monitoring sites in Ireland over different periods: 5 years (2018-2022), 10 years (2013-2022), 15 years (2008-2022), and the available years of data for each site. In the coastal regions, Mace Head shows a consistent decrease in O_3 levels over the 5, 10, and 15-year periods, although the entire dataset exhibits a small rising trend 0.02 µg/m³ per year. These trends are mostly in agreement with previous studies, where there was a positive trend observed in

296 background O_3 up to the mid-2000s, which stabilised and began to decline in the 2010s
297 (Derwent et al., 2018). Valentia shows a long-term decreasing trend of -0.23 μg/m³ per year,
298 consistent with the previous study by Tripathi et al..2010.

299 In rural areas, Monaghan exhibits a declining trend in O_3 concentrations across all time
300 periods, indicating an overall reduction. Laois shows an upward trend over the 10 and 15-
301 year periods, though there is a slight decline in the most recent 5 years. Kilkenny presents
302 slight negative trends over the 5 and 10-year periods (-0.29 and -0.01μg/m³ per year).
303 Negative trends are observed in Castlebar-(0.71 and -0.05 μg/m³ per year).

304 The Dublin urban area sites (Rathmines, Clonskeagh, Swords) predominantly show increasing
305 trends in O_3 levels, indicative of changes in urban pollution or local emissions, with decreased
306 suppression of O_3 levels in urban regions due to decreased local emissions. (Derwent et al.,
307 2024). This is consistent with the "weekend effect," as observed by Atkinson-Palombo et al.
308 (2006) whereby a reduction in NO_x due to reduced weekend traffic decreases O_3 removal by
309 NO_x titration, leading to higher surface O_3 levels, likely to occur in wintertime, and in regions
310 with low photochemical production due to low insolation and temperatures, as observed in
311 Ireland. It is duly noted that NO_x driven O_3 removal dominates over photochemical production
312 in these sites. A comparable study in the UK carried out by Finch and Palmer (2020) attributed
313 similarly rising trends in surface O_3 between 1999 and 2019 to decreasing NO_x, characterising
314 UK observation sites as VOC-limited. Mixed results are observed at the urban stations of Cork,
315 with a positive trend at the South-link Road and Bishopstown, but a negative trend at the UCC
316 station. The UCC station, although classified as urban, lies within the university campus;
317 hence, it would not be subject to significant local emissions. Coastal sites like Mace Head and
318 Valentia generally show decreasing trends, potentially due to less local emission sources but
319 with more significant impacts from regional and long-range transport, However, a detailed
320 analysis of the trends requires consideration of seasonal effects.

Previous studies indicate that in northeast Europe, peak surface ozone concentrations have generally declined, reflecting the effectiveness of emission control measures (Yan et al., 2018). In contrast, background and lower-level O_3 concentrations have continued to increase, particularly at rural and suburban sites. Consistent with this, urban observations from 2000–2021 show increasing trends in median and lower-percentile O_3 levels, while the highest extremes have mostly decreased (Nelson et al., 2025).

Table 2. - Trends in surface O_3 concentration (µg/m³ per year) calculated for 13 sites in Ireland over different periods over the complete dataset: 5 years (2018-2022), 10 years (2013-2022), 15 years (2008-2022), and the available measurement record for the site. The p-value evaluates the reliability of the trend, whereas a lower p-value indicates trend certainty. Adopting the trend reliability scale defined for TOAR-II studies (Chang et al., 2023), trends with very high certainty will be marked by ***($p \leq 0.001$), trends with high certainty with ** ($p \leq 0.01$), and low to medium certainty with *($p \leq 0.05$).

Site No	Site name (Classification)	Measurement Record	Trend over record µg/m³ per year	5-year trend 2018-2022 µg/m³ per year	10-year trend 2013-2022 µg/m³ per year	15-year trend 2008-2022 µg/m³ per year
1	Mace Head (C)	1994-2022	0.02	-0.25	-0.31***	-0.11*
2	Valentia (C)	2001-2022	-0.23****	-1.15****	-0.84****	-0.32***
3	Monaghan (R)	1995-2022	-0.19****	-0.74**	-0.35**	-0.09*
4	Laois (R)	2005-2022	0.39****	-0.15	0.3**	0.46****
5	Kilkenny (R)	2012-2022	0.02	-0.29	-0.01	

6	Castlebar (R)	2009-2022	0.18**	-0.71**	-0.05	
7	Rathmines (U)	2002-2022	0.27****	1.72****	1.15****	0.48****
8	Clonskeagh (U)	2008-2022	0.33****	0.97***	0.12	0.33****
9	Swords (U)	2009-2022	0.6****	0.07	0.33****	
10	Wicklow Bray (U)	2009-2022	0.14*	0.04		
11	Cork Southlink Road (U)	2014-2022	0.51*	-0.44		
12	Cork Bishopstown (U)	2016-2022	1.05***	-1.81*		
13	Cork UCC (U)	2018-2022	-0.94	-0.94		

337

338

339 **3.2.2 Monthly trend**

340 Figure 3. shows the monthly trend for 10 years from the period 2012-2022. Mace Head
341 (coastal) and Monaghan (rural) sites predominantly show a rising trend in winter/early spring,
342 with a decreasing trend in late spring to summer. Valentia shows a decreasing trend in every
343 month except February when levels are significantly impacted by long-range transport and
344 stratospheric sources (Auvray and Bey, 2005; Pan et al., 2018). Urban sites show a general
345 increasing monthly trend, as yearly trend but with a seasonal signal in Clonskeagh with an
346 increase in winter-spring and a decrease in late spring or summer. Laois is characterised as a
347 rural site yet exhibits rising trends similar to the urban sites for all months except December,
348 indicating that the measurement station is affected by nearby emissions. Seasonal trends of the
349 15-year dataset are supplied in supplementary Figure S2, where coastal stations exhibit a
350 pronounced increase in late winter, and a decrease in late summer, with a consistent near-year-
351 round increase in Rathmines and Laois.

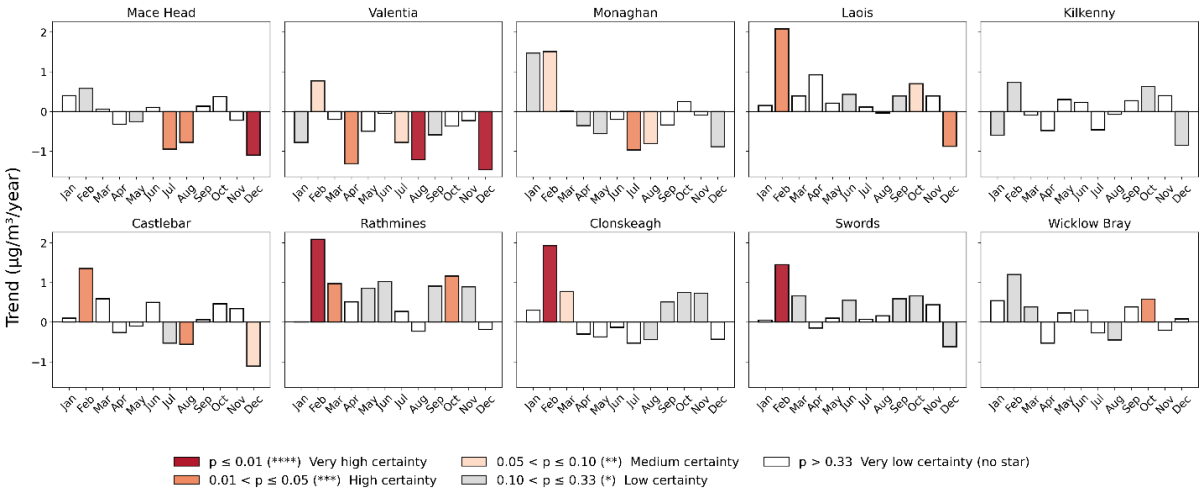

352

353 **Figure 3.** Monthly trend analysis of O_3 at different sites for 10 year period. (2012-2022)
354 Adopting the trend reliability scale defined for TOAR-II studies (Chang et al., 2023), trends
355 significance highlighted by colour.

356 ### 3.3 O_3 Exceedance

357 The O_3 exceedances at 13 sites in Ireland over the available measurement dataset are identified
358 according to WHO criteria, and the results are shown in Figure 4. The highest and lowest
359 numbers of O_3 exceedances were observed at Mace Head and Rathmines, representing coastal
360 and urban sites, respectively. Most exceedances occurred in spring (March, April, May),
361 coinciding with the spring-time maximum. Rathmines had its highest number of exceedances
362 in April 2019, while Laois reached a peak of 13 exceedances in May 2017. Castlebar and
363 Swords show increased exceedance occurrences in spring and early summer, particularly
364 notable spikes occurring in 2010, 2013, 2016, and 2019. Conversely, Wicklow Bray exhibited
365 a different pattern, showing significant spikes in February and March 2022, alongside
366 occasional exceedances during March, April, and May, for example, in 2012 and 2018. Cork
367 South link Road also recorded exceedances, particularly in March and notably in June. Cork
368 Bishoptown shows exceedances, especially in February and March 2019, while Cork UCC
369 recorded exceedances in April and May 2019. Kilkenny consistently exhibited exceedances

during spring and summer, with April and May often recording the highest numbers, particularly in 2019. This highlights the impact of seasonal atmospheric conditions on O_3 levels. It is noted that summertime exceedances, although less frequent in occurrence, indicate photochemical production events that would be required to elevate O_3 levels from the annual dip in the seasonal cycle to exceed the WHO AQG threshold. These episodic spikes are characteristic of unique climatic or pollution events and warrant further study.

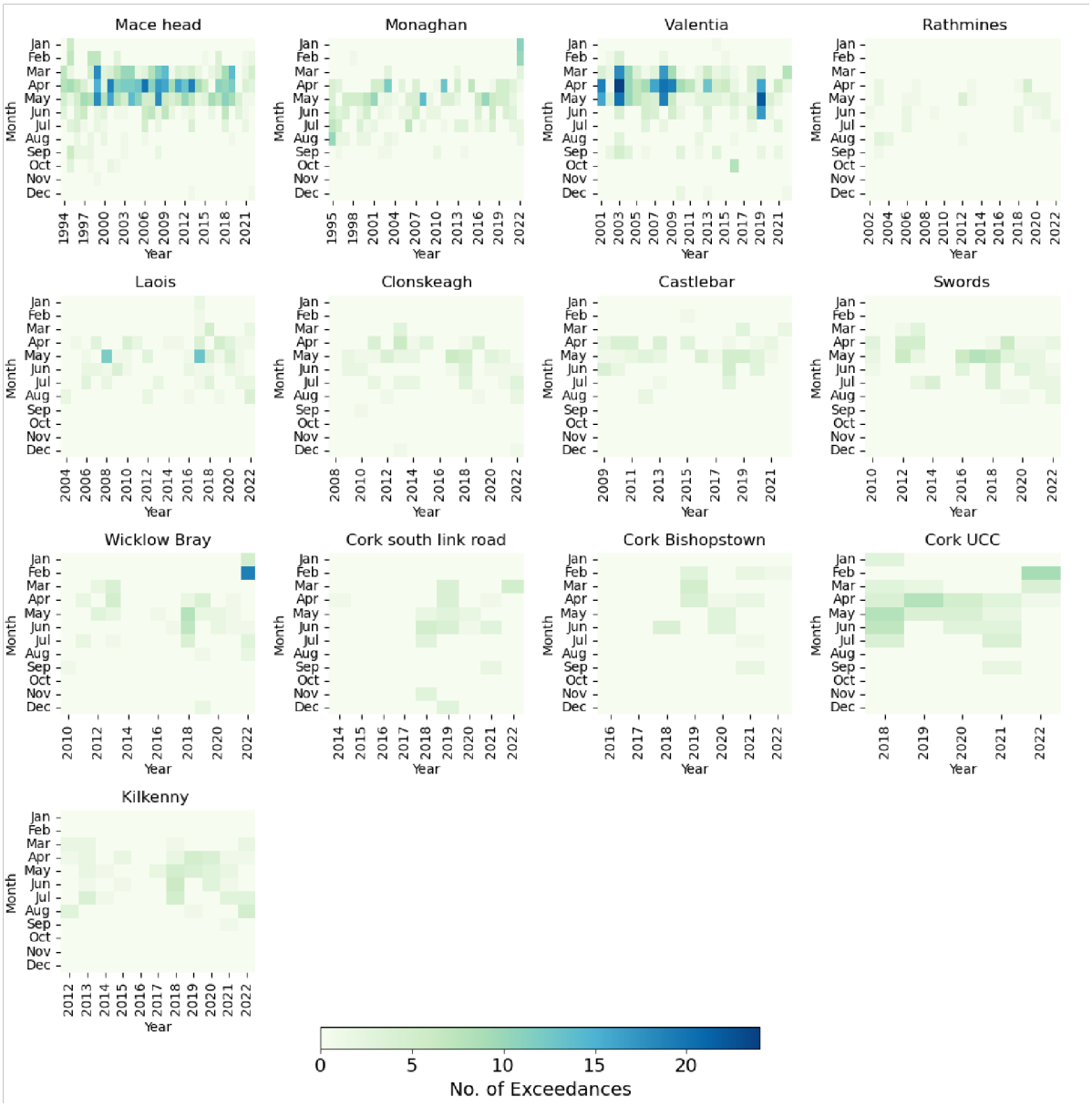

Figure 4. - Monthly O_3 exceedance at different sites in Ireland. Exceedances are defined as days on which the maximum 8-hour running average of ozone (O_3) exceeds 100 µg/m³.

Figure 5 depicts trends in NO_2 and CH_4 concentrations across various Irish measurement sites. NO_2 trend calculations are based on site-specific data periods, Cork South link Road (2014–2022), Ballyfermot (2003–2022), Davit Road (2018–2023), Rathmines (1995–2024), Swords (2011–2025), Laois (2014–2026), Castlebar (2003–2027), Louth Dundalk (2019–2028), and Monaghan (2001–2029). For CH_4, the data cover the period 2010–2022. Most monitored sites exhibit a decreasing trend in NO_2 concentrations, most likely in response to pollution control on transportation, industrial activities, and energy production in the EU and North America (Coleman et al., 2013; Donlon et al., 2024). In contrast, CH_4 levels observed at three sites - Mace Head, Malin Head, and Carnsore Point indicate a significant and persistent rise in CH_4 concentrations. Mace Head is known for its clean Atlantic air and Malin Head, situated at Ireland's northern tip near the UK border, offers a unique position to observe both clean marine air and transboundary pollution, whereas Carnsore Point in the southeast captures air masses from both the UK and mainland Europe (Spohn et al., 2022). These NO_2 and CH_4 trends reveal a dual dynamic: while NO_2 levels are decreasing due to effective emission controls, CH_4 levels relentlessly rise, highlighting the need for enhanced mitigation strategies targeting CH_4.

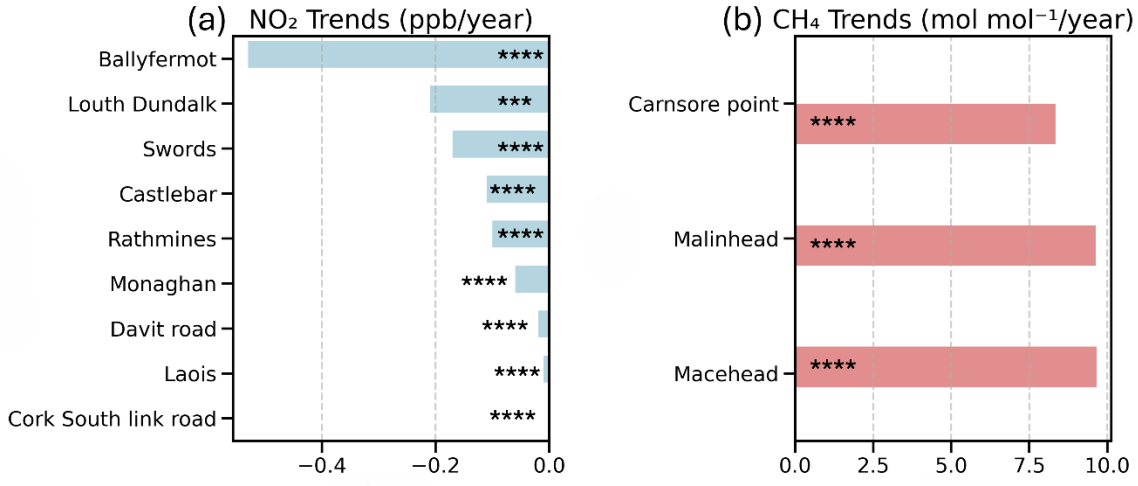

Figure 5. Trend in O_3 precursors NO_2 (a), and CH_4 (b) at different sites. Statistical significance of trend is indicated, increasing * with increasing trend reliability, as in Table 1.

To evaluate the relationship between NO_x and O_3 concentrations in an Irish context and the potential benefit of abrupt enforcement of NO_x control measures, we assess the impact of the COVID-19 2020 lockdown, Spring 2020, whereby the lockdown period saw a prominent relative decrease in NO_2, yet an increase in surface O_3 compared to average measurements for the same months 2017-2019 in most national monitoring stations (Figure 6). The negative correlation between O_3 and NO_2 is indicative of a NO_x-saturated regime, normally associated with polluted urban environments and NO_x titration events. Analysis of the impact of the lockdown on Irish O_3 is discussed by Spohn et al. (2022), and a similar O_3 decrease was widely observed across Europe during the COVID lockdown (Ordóñez et al., 2020; Tavella & da Silva Júnior, 2021; C. Zhang & Stevenson, 2022). Significant enhancement of O_3 occurs at the inland measurement sites, despite a 2020 springtime decrease in O_3 observed at background coastal sites, Mace Head and Valentia. These coastal stations are less sensitive to changes in European NO_x emissions than inland sites and more sensitive to stratospheric and hemispheric transport (Tan et al., 2018). It is noted that April and May 2020 had unique meteorological conditions compared to previous years, with lower wind speed, less rain and significantly higher solar radiation, see Figure 12 in Spohn et al. (2022). These meteorological conditions would potentially facilitate photochemical O_3 production, contributing to positive O_3 anomalies during the lockdown period in addition to NO_x reduction, also potentially enhancing dry deposition to the ocean. Further investigation into this topic would warrant model sensitivity studies, beyond the scope of this current work.

The negative correlation between NO_x and O_3 under relatively clean atmospheric conditions indicates that O_3 levels are influenced predominantly by transport and chemical removal, and local photochemical production does not represent a significant surface O_3 source owing to

periods of low-insolation periods and low temperature, which are characteristic of Irish meteorology and frequent cloud cover (Pallé and Butler, 2002)

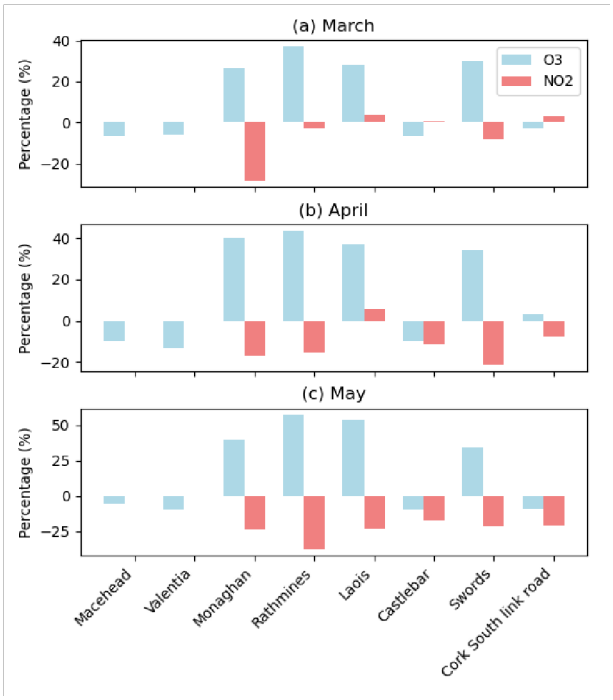

Figure 6. Percentage change in NO_2 and O_3 during the lockdown period of 2020 as compared to the 2017-2019 average at different sites in Ireland for (a) March (b) April (c) May.

3.4 Model and Observations Comparison

3.4.1 Comparison between CAM4 – Chem Model and Observations

Global simulations were performed with the CAM4-Chem model enabled with source tagging (Butler et al., 2018) for 2000-2018 and the modelled O_3 over Ireland was compared with surface O_3 measurements at five sites. The grid details are shown in Figure S5. This model has already been comprehensively evaluated on a global scale (Nalam et al., 2025) against the TOAR-1 dataset, whereby the model performed well, albeit with a high bias attributable to the model's coarse resolution and implications for the resolution of urban chemistry (Ansari et al., 2025). Figure 7 shows the comparison of monthly O_3 CAM4-Chem and ground station O_3 data.

436 From this figure, it is observed that CAM4-Chem exhibits negative (positive) bias in rural and
437 coastal (urban) sites. The underestimation at Mace Head is probably caused by the coarse grid
438 resolution, covering a large area not representative of Mace Head conditions.

439 The influence of coastal meteorology, which suppresses O_3 formation due to cooler
440 temperatures and persistent cloud cover (McVeigh et al., 2010), also leads to an
441 underestimation of O_3 (Yerramilli et al, 2012). The dry deposition rate over land would exceed
442 that over the ocean, leading to a lower simulated O_3 concentration for the grid cell which covers
443 both land and ocean surface. Dry deposition is enhanced by solar radiation (Coleman et
444 al.,2012; Coleman et al., 2013; Pio et al., 2000) hence model measurement discrepancy is at a
445 maximum in late summer months. As outlined by Fiore et al. (2009), models average the
446 landscape characteristics within a grid cell, which can enhance O_3 deposition and result in
447 lower simulated O_3 concentrations; hence, the discrepancy is more pronounced in the clean
448 sector data.

449 Overestimation of O_3 in Clonskeagh and Cork South link Road is likely due to coarse grid
450 handling of localised emissions and subsequent atmospheric chemistry.

451

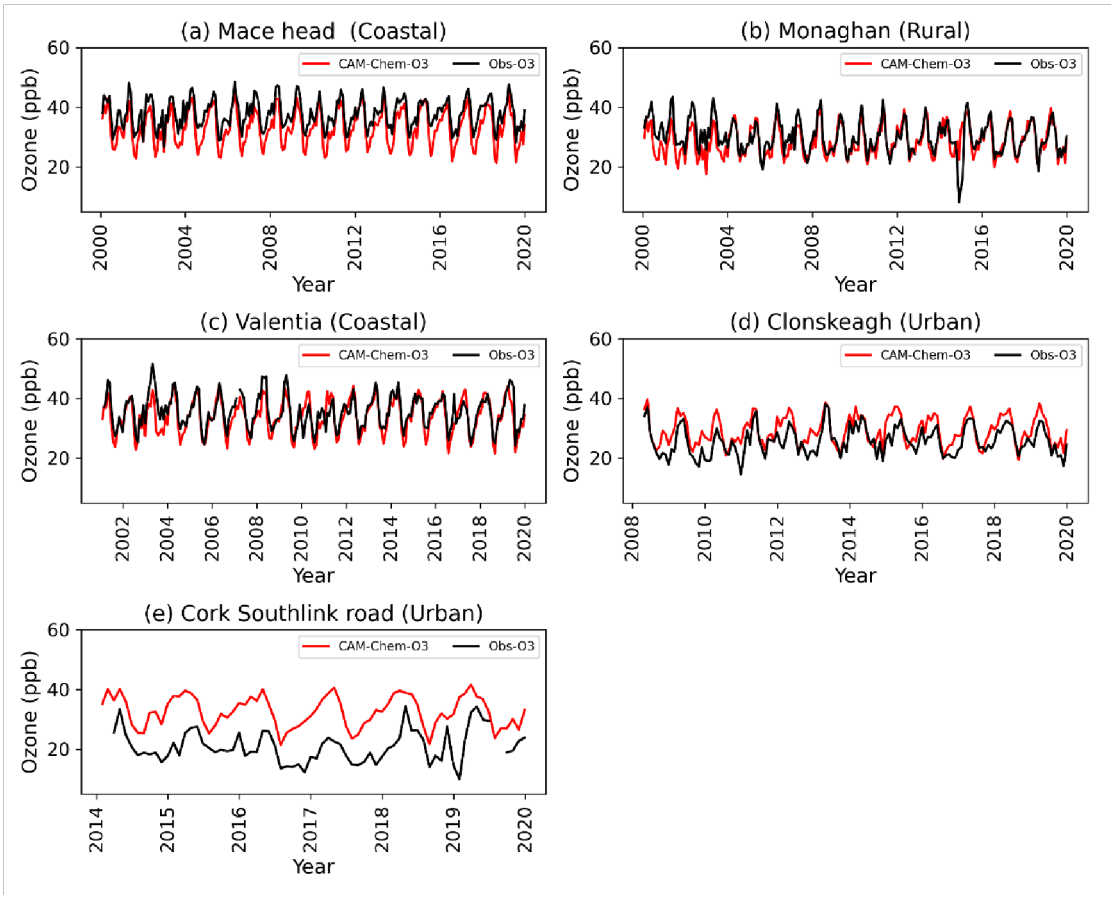

Figure 7. The comparison of Monthly CAM4 – Chem O_3 and Monthly O_3 observations at five sites in Ireland**.**

At Mace Head, the model shows a negative mean bias of - 4.42 (-11.68% normalized mean bias) but strong correlation (r =0.83). In Monaghan and Valentia, the model shows smaller biases of −1.43 and −1.54, normalized mean biases of −4.74% and −1.54%, and correlation coefficients of 0.73 and 0.72, respectively. These high correlations are in line with (Tilmes et al., 2015). However, at Clonskeagh and Cork South Link Road, the model overestimates, with positive biases (3.38 and 11.98) and weaker correlations (0.68 and 0.49). Statistics are given in more detail in the supplementary material Table S1. These results suggest better model performance at coastal/rural sites and greater discrepancies in areas affected by local sources, as expected at this model resolution.

3.4.2 Source attribution using CAM4-Chem

To quantify the contribution of various precursor emission sources to modelled O_3 concentrations, the TOAST1.0 dual NO_x and VOC tagging technique was utilised (Butler et al., 2018). This allows attribution of modelled O_3 to the emissions of NO_x and VOC precursors across different source sectors and geographical regions as listed in Table 3.

Table 3. - List of tags used in NO_x and VOC tagging.

Regional Land-Based Tags		**Regional Oceanic Tags**		**Global Sector/ProcessBased Tags**	
ARC	Arctic	**NAL**	North Atlantic	**AIR**	Aircraft
CAS	Central Asia	**ENA**	Eastern North Atlantic	**BIO**	Biogenic
EAS	East Asia	**NAE**	North America East Coast	**BMB**	Biomass Burning
EUR	Europe	**NAW**	North American West Coast	**LGT**	Lightning
MCA	Mexico & Central America	**NPA**	North Pacific	**STR**	Stratospheric Intrusion
MDE	Middle East	**BNS**	Baltic and North Seas	**XTR**	Extra untagged O_3

NAF	North Africa	**HBY**	Hudson Bay	**CH4**	Methane
NAM	North America	**IDO**	Indian Ocean	**OCN**	Oceanic Sources (DMS)
RBU	Russia-BelarusUkraine	**MBC**	Mediterranean, Black, and Caspian Seas	**SHP**	Shipping
SAS	South Asia	**SHO**	Southern hemispheric oceans	**AIR**	Aircraft
SEA	Southeast Asia			**INI**	InitialConditionO_3
VRW	Rest of the World				

The monthly tagged major precursor contributions to surface O_3 at Mace Head, averaged over the 2000-2018 simulation period, are shown in Figure 8. The stratospheric source of O_3 dominates in Winter-Spring, contributing to the spring-time maxima due to vigorous stratospheric transport. European NO_x emissions contribution peaks in May, while lightning NO_x has the greatest impact in winter. North American (NAM) NO_x emissions contribute 3.5 to 5.25 ppb, comparable to European NO_x, but with an earlier peak in April. Aviation emissions contribute 1 to 3 ppb, with the highest contributions in winter and spring. Biogenic NO_x, significant between June and October, contributes an average of 3.6 ppb, with higher contributions during August and September. O_3 derived from biogenic VOC sources average over 4 ppb during late autumn, maintaining a more sustained contribution throughout the year. East Asian NO_x emissions, contribute up to 3.6 ppb, with a minimum contribution in July and August. North Atlantic shipping NO_x (NAL) accounts for up to 2.4 ppb of O_3 during July. The total shipping NO_x (SHIP) also contributes significantly It is the addition of all oceanic emissions and shows the highest contribution in June.

Methane (CH_4) is the dominant reactive carbon molecule contributing to O_3 formation. VOC emissions from biomass burning also play a measurable role, contributing 1 to 2 ppb, with

their largest contributions in August and September. Finally, European VOC emissions contribute 1 to 3 ppb, with the largest impact from March to May, coinciding with the spring-time peak in surface O_3.

These findings allow quantification of specific sources amidst the complex interplay of regional and global sources in driving seasonal variations in surface O_3 levels over the Irish domain, highlighting the roles of stratospheric processes, anthropogenic emissions, biogenic sources, and lower-latitude contributions in shaping the observed patterns at background monitoring sites such as Mace Head.

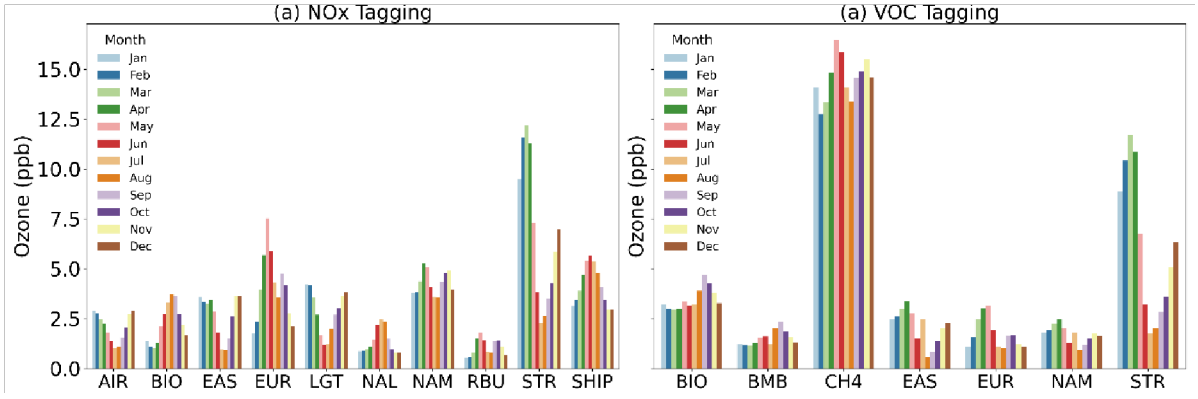

Figure 8.- Absolute contribution of major NO_x sources (a) (NO_x Tagging) and VOC source (b) (NO_x Tagging) to the CAM4-Chem simulated surface O_3 for the Mace Head grid cell between 2000-2018.

Figure 9 shows the monthly changes in contributions to surface O_3 at Mace Head over the simulation period (2000-2018). A negative (blue) trend indicates that the contribution of the source to simulated surface O_3 in this grid cell has declined over the simulation period, whereas a positive trend (red) indicates the contribution to surface O_3 has risen. Figure 9 (a) shows that simulated O_3 at Mace Head originating from European or North American NO_x decreases over the simulation period, consistent with EU & North American emission reductions (Guerreiro

et al., 2014). More significant reduction occurs in late Spring through late summer, when EU NO_x contributions are most significant to Mace Head O_3 concentrations (as seen in Figure 8).

There is a rising trend in simulated surface O_3 originating from NO_x emissions from global aviation, from East Asia, and to a lesser extent from South Asia, which is more pronounced in the wintertime. Wintertime temperatures in South Asia are still high enough to sufficiently produce local ozone, especially when NO_x emissions are rising (Crippa et al., 2023). The relatively longer, atmospheric lifetime of O_3 in the free troposphere during winter enables longer-range intercontinental transport (Huang et al., 2017;Yu et al., 2013). This seasonality in source contributions explains the observed reduction in spring-time maxima and increase in winter-time levels from the measurement record. EastAsian and South-Asian VOCs also contribute to a rising trend in simulated O_3, with a more pronounced increase in winter and spring. This highlights a different pattern in hemispheric O_3 contributions, where EU and NAM emission reductions coincide with increased contribution from lower latitudes which could potentially become a more significant source of background O_3 in the Northern Hemisphere in the future. The contribution of CH_4 also has a positive trend over the simulation period, but the CH_4 trend has a reliable correlation only in December and spring periods, with very low certainty in CH_4 contribution trends for summer months (correlation coefficient, $p>0.33$). Contribution to simulated O_3 at Mace Head from EU and NAM anthropogenic VOC show a negative trend for all months, consistent with trends from EU and NAM anthropogenic NO_x.

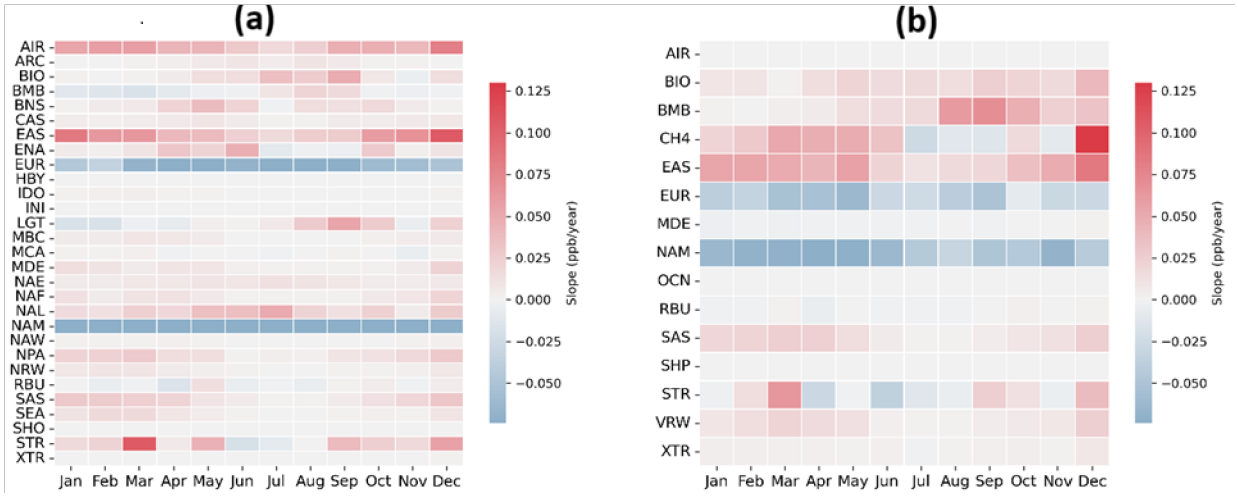

Figure 9. Trends in contributions to monthly average modelled Mace Head grid cell surface O_3 for the 2000-2018 period derived from (a) NO_x tagging and (b)VOC tagging.

Table 4. shows the overall trend in the main contributors to NO_x and VOC tagging. It is observed that there is an increase in simulated surface O_3 originating from NO_x contributions from aviation and East Asia, while there is a decrease in European (EUR) and North American (NAM) NO_x contributions. In VOC tagging, Methane (CH_4) and East Asian anthropogenic VOC (EAS) contribute to a rising trend over the simulation period, whereas anthropogenic VOC contributions from Europe (EUR) and North America (NAM) show a negative trend.

Table 4 - Overall Trend in contributions to Mace Head grid cell O_3 simulated by CAM4-Chem for NO_x tagging and VOC tagging over the simulation period in units of ppb per year. reliability scale defined for TOAR-II studies (Chang et al., 2023), Statistical significance of trend is indicated using star notation: **** denotes $p \leq 0.01$ (very high certainty), *** denotes $0.01 < p \leq 0.05$ (high certainty), ** denotes $0.05 < p \leq 0.10$ (medium certainty), * denotes $0.10 < p \leq 0.33$ (low certainty), and no star denotes $p > 0.33$ (very low certainty).

NO_x Tagging		**VOC Tagging**	
	Slope (ppb/year)		Slope (ppb/year)

AIR	0.0467****	CH_4	0.0590****
EAS	0.0491****	EAS	0.0333****
EUR	-0.0900****	EUR	-0.0553****
NAM	-0.1243****	NAM	-0.0670****

546

547 **3.5 O_3 Trends in Background and EU influenced sector Airmasses at Mace Head**

548 Although Mace Head is classified as a global background site, quantification of the baseline
549 pollution levels requires trajectory analysis, whereby both measured and modelled data is
550 filtered to limit the data to that arriving from the clean sector, unaffected by land-based
551 emission sources, as discussed in Section 2.2. Figure 10 displays trends in observed and
552 simulated O_3 at Mace Head, separated into seasons and clean/EU influenced sectors according
553 to the trajectory analysis. The figure shows that the clean sector has consistently higher O_3
554 concentrations than the EU influenced sector for Winter, Spring and Autumn, with the most
555 significant disparity between clean and EU sectors in winter/spring when stratospheric
556 intrusion and lightning NO_x contribute most significantly to O_3, as discussed in Section 3.4.2.
557 O_3 originating from EU airmasses is susceptible to higher rates of dry deposition and removal
558 via local pollution while traversing the land-mass westwards towards Mace Head, leading to
559 higher O_3 in clean-sector air masses consistent with previous studies (Coleman et al., 2013). A
560 decreasing trend in mean spring-time levels is observed for both clean and EU influenced
561 sectors, consistent with the sustained decrease in precursor emissions in Europe and North
562 America as displayed in Figure 9.An increasing trend (0.26 ppb/year) is observed in the winter-
563 time EU influenced sector, with a trend of smaller magnitude (0.08 ppb/year) observed in the
564 clean sector, indicating a decrease in winter-time O_3 depletion events due to decreasing

565 European emissions (from the EU influenced sector), consistent with the conclusions from
566 previous studies of Mace Head surface O_3 (Derwent et al., 2024). Summer-time values do not
567 exhibit a notable trend or a discrepancy between the clean and EU influenced sector
568 measurements, indicating that there is little O_3 advected into Europe from the west in the
569 summer months. It is noted that the seasonal trends exhibit slopes with p-values ranging
570 between $0.1 > p > 0.01$, which denote trends of medium to high certainty, as defined by TOAR
571 assessment criteria of Chang et al., 2023.

572 Although the model results display a negative bias for reasons outlined in section 3.4.1, the
573 clean sector consistently exhibits higher simulated O_3 concentrations than the EU-influenced
574 sector, except during the summer season. In the winter season, a significant increasing trend is
575 observed for simulated O_3 from both sectors, aligning with observations. A decreasing trend is
576 observed during the summer season, again consistent with the observations for both sectors. In
577 spring and autumn, modelled O_3 exhibits a positive trend over the simulation period.

578 Trends in contributors of model O_3 during the different seasons for the clean and EU-influenced
579 sector are shown in Tables S3 to S4 in the supplementary material. Aviation and East Asian
580 NO_x show consistently positive and significant trends in both sectors, while North America
581 NO_x shows strong negative trends throughout the year in the clean sector. For the EU-
582 influenced sector in NO_x tagged (Table S2), similar positive trends observed for aviation and
583 East Asian, with North America NO_x remaining negative and European NO_x showing more
584 significant declines in spring and winter. In case of VOC tagged O_3, the East Asian VOCs
585 shows an increasing trend and North America VOCs show a negative across all seasons in both
586 sectors (Table S3 and S4). European VOCs also show a consistent negative trend, particularly
587 strong in the EU-influenced sector. Methane trends are seasonally positive, especially in spring
588 and winter.

589 It is observed that the model consistently simulates O_3 at lower concentrations than that
590 observed at Mace Head. This is not surprising, considering the coarse resolution of the model,
591 which limits its ability to represent fine-scale processes and dry deposition accurately. Dry
592 deposition is typically higher over land, and the grid cell covering Mace Head includes land
593 area, as shown in Figure S5 of the supplementary material. Further, as explained by Fiore et
594 al. (2009), models average the landscape characteristics within a grid cell, which can enhance
595 O_3 deposition and result in lower simulated O_3 concentrations; hence, the discrepancy is more
596 pronounced in the clean sector data.

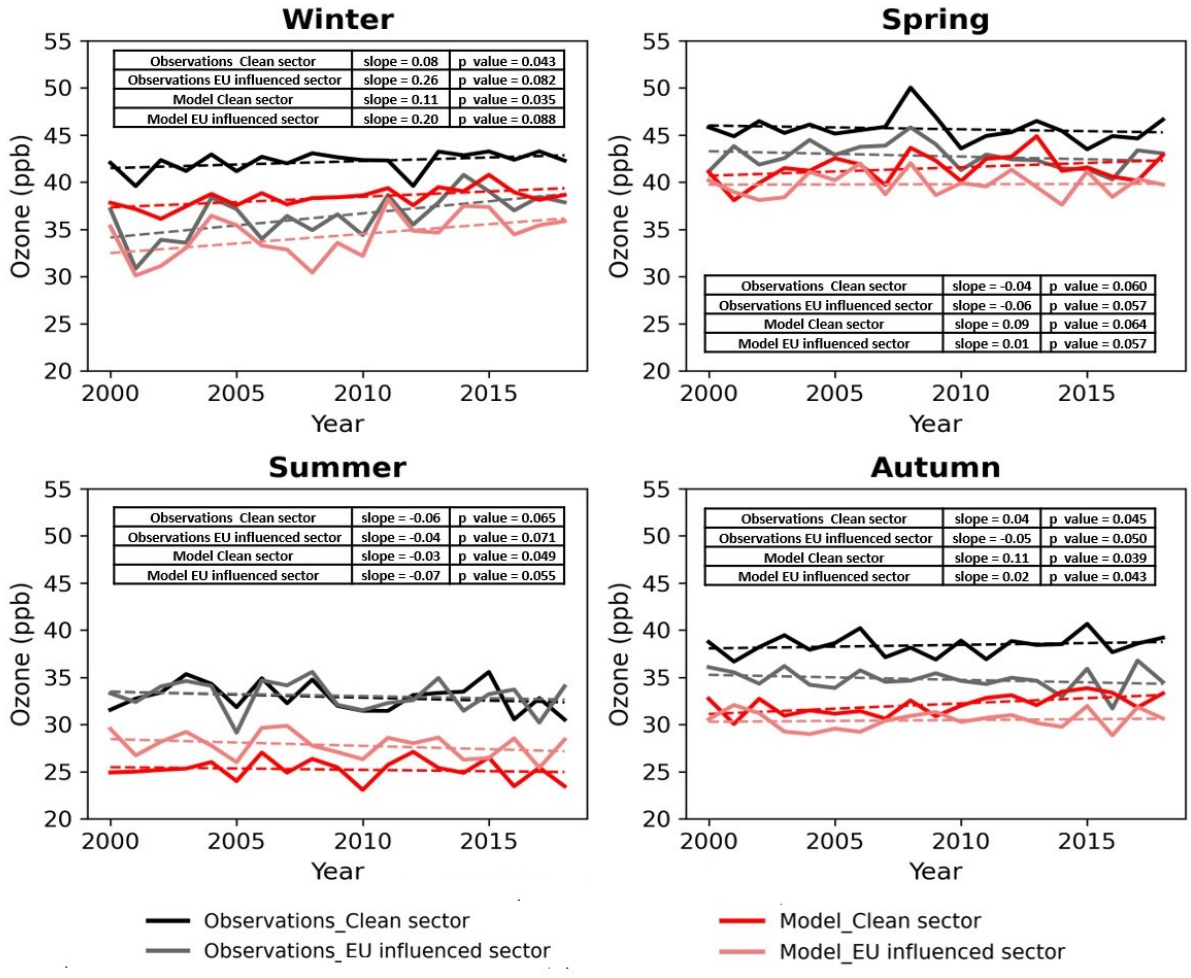

597

598 **Figure 10.** - Trend in seasonal Average of observed O_3 (black) and Model O_3 (red) at Mace
599 head, separated into clean sector and EU-influenced sector.

3.6 Exceedances from the clean and EU-influenced sector at Mace Head

Exceedances observed at Mace Head between 2000 and 2022 are separated into clean and EU-influenced sectors based on trajectory air masses and shown in Figure 11. 35% of all exceedances for this period occurred in clean air masses, the remainder occurring when air masses include EU outflow and contribution from local sources to enhance surface O_3 at Mace Head, which is already elevated compared to inland and urban sites. It is notable that there is a higher proportion of exceedances that occur from EU- influenced sector, despite higher mean observations from the clean sector for all seasons. This occurs because of an enhancement of surface O_3 occur during an influx of polluted air from the EU, UK or local sources. The EU influence on exceedance becomes more proportionally prominent in late Spring and summer, with more frequent easterly airflow when there is a higher occurrence of stagnation events.

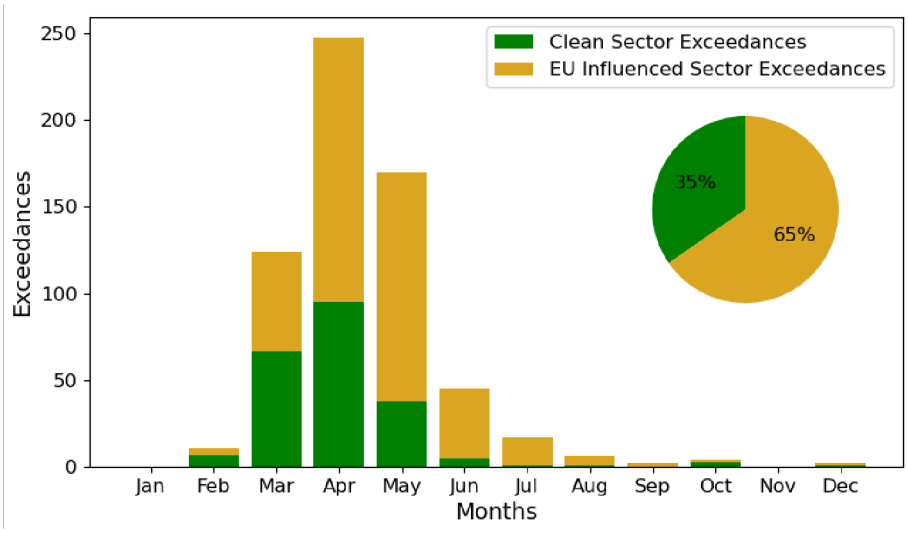

Figure 11. - Exceedances measured at Mace Head per month from 2000 until 2022, during the clean air sector(green) and EU influenced sector (yellow). The percentage of both to total exceedances is shown in the inlay.

Figure 12 shows the trend in spring-time exceedances and the 95th percentile Springtime O_3 measured at Mace Head between 2000 and 2022. A decreasing trend in exceedances is observed, with a greater decreasing trend from the EU and the locally influenced sector. This indicates that the changes that are driving the reduction in the exceedances in Europe are coming into effect at a quicker rate than the changes that are driving the O_3 event reduction over the North Atlantic. The trends in the exceedance counts are not significant, according to the criteria in Chang et al., 2023, but there is a statistically significant decreasing trend in the 95th percentile springtime surface O_3 over the measurement record. Figure 12 (b) shows the trend in spring-time surface O_3 measured at Mace Head segregated into the Clean and EU-influenced sector. The trend is more significant both in magnitude and statistical certainty for the EU-influenced sector, indicating that European emission changes have a more pronounced effect on springtime O_3 measured at Mace Head O_3 as compared to changes affecting O_3 transported or formed over the North Atlantic.

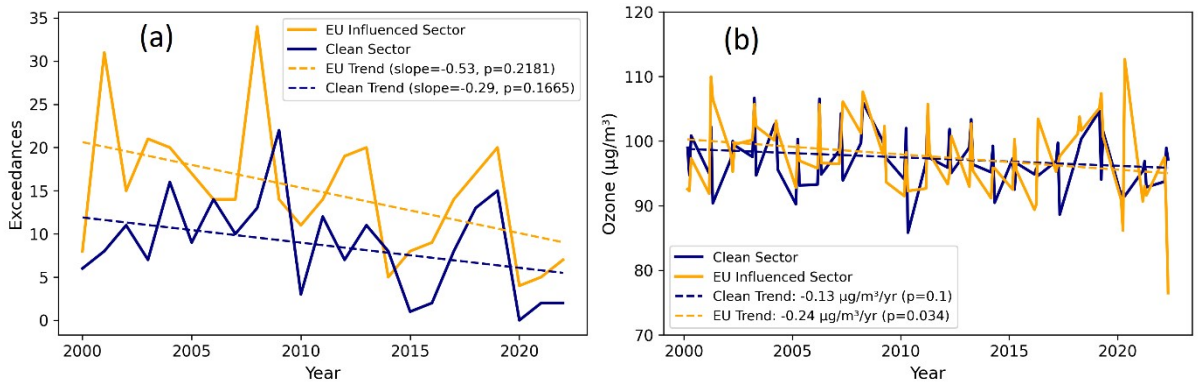

Figure 12. (a) The trend in Spring-time exceedances measured at Mace Head between 2000 and 2022 (blue) with the clean-air exceedances (gold), and (b) The trend in the 95th percentile of spring (Mar- May) O_3 measured in µg /m^3 for the clean sector (blue) and the EU-influenced sector (gold).

Figure 13 shows monthly cumulative contributions to simulated O_3 concentrations within the Mace Head grid cell for NO_x and VOC tagging during O_3 exceedance. First, the exceedances

were identified from O_3 observations as discussed in Section 3.3 and then these exceedances were divided into two sectors the EU-influenced sector and the clean sector. In Figure 13, the hourly O_3 exceedance cumulative concentrations in ppb, along with the contributions from different parameters, are shown. It indicates which parameters contribute more to the exceedances, in both the EU-influenced sector or the clean sector. In this, the $\mu g/m^3$-to-ppb conversion is applied to the exceedances.

These exceedances are categorised into clean and EU-influenced sectors. The maximum exceedances are observed in March to May. From Figure 13 (a), it is clear that stratospheric intrusion, North American NO_x, European NO_x, and East Asian NO_x are the major contributors driving exceedances at Mace Head during the spring months (March to May). European emissions dominate the supply of NO_x precursors in April, reaching their peak in May. Figure 13 (b) shows that CH_4 is the most dominant VOC source, followed by stratospheric intrusion and Biomass burning. North American and European VOC emissions also contribute significantly to O_3 formation during this period. Collectively, these findings highlight the complex interplay of regional and global sources in driving surface O_3 exceedances over the Irish domain.

North American NO_x also contributes significantly to exceedance in both clean and EU-influenced sectors at Mace Head during March to May month, likely due to long-range transport and mixing, regional stagnation or synoptic-scale recirculation. In the case of VOC tagging, stratospheric intrusion, and CH_4 show notable contributions. Biomass burning, East Asian emissions and North American VOC emissions also play a role in O_3 exceedances. The IN_SHIP indicates the total contribution of all international shipping emissions (ENA,NAE,NAW,NPA,BNS,HBY,IDO,MBC,SHO) which is significant in April and May.

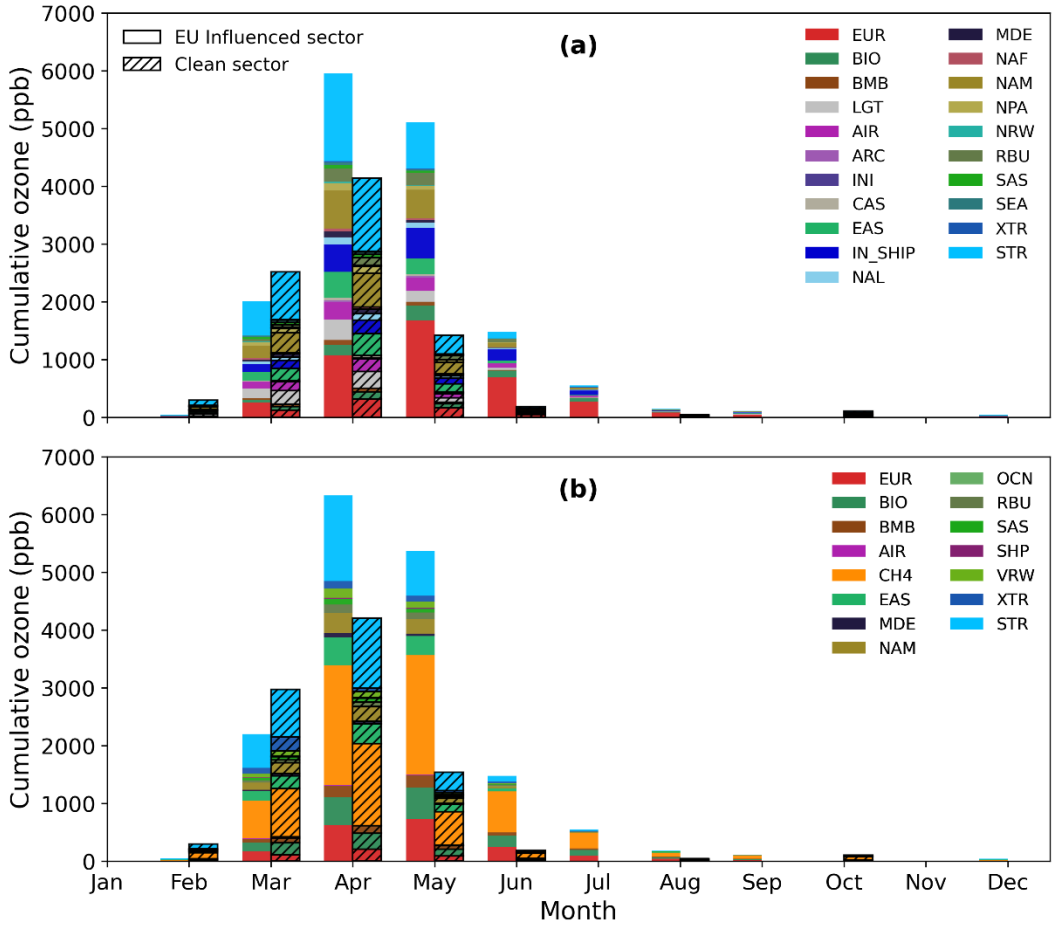

Figure 13 -Monthly cumulative Mace Head grid cell O_3 contributions to EU influenced sector and clean sector exceedances (a) NO_x tagging and (b) VOC tagging Mace Head grid cell.

4. Conclusion

This study highlights the complexities of O_3 pollution in Ireland, revealing that coastal areas experience higher O_3 concentrations than rural and urban environments, attributed to the effect of transboundary pollution and stratospheric intrusion. Over the last two decades, urban sites have shown a significant increasing trend in O_3 levels, particularly in winter, influenced by decreasing anthropogenic pollution in Europe, the UK, North America and local to the observation sites, representing a decline in chemical removal mechanism (Derwent et al., 2024; Simmonds and Derwent, 1991). The analysis also points out that the majority of exceedances at coastal monitoring sites coincide with the annual spring maxima. Using the advanced capabilities of the CAM4-Chem model with dual NO_x and VOC tagging, we identified key

672 factors affecting seasonal O_3 variations, such as the spring-time peak and summer dip, driven
673 by a mix of stratospheric intrusion, NO_x emissions from lightning, long range and hemispheric
674 transport, regional emissions and aviation related emissions. Trend analysis from simulation
675 results identified East Asian and aviation emissions as significant contributors to the rising
676 winter trends in O_3, while reductions in North American and European emissions accounted
677 for the decrease in spring peaks. This study provides a comprehensive understanding of the
678 various factors affecting O_3 levels in Ireland, offering important insights for the development
679 of O_3 pollution control policies.

680

681 **Data availability**

682 All data are available upon request.

683

684 **Author contributions**

685 LC designed the study. NK analyzed the data and wrote the manuscript. TA and TB provided
686 CAM-Chem model results and reviewed the manuscript. EC contributed to the air mass
687 trajectories analysis. JO, CD and DM reviewed the manuscript and edited it. LC edited it
688 with contributions from all coauthors **.**

689 **Competing interests**

690 The authors declare that at least one of the authors sits on the editorial board of ACP.

691 **Acknowledgement -** The authors acknowledge the Environmental Protection Agency (EPA)
692 of Ireland for their financial support of the Ozone project under the EPA Research
693 Programme.
694 2021-2030 (project number 2022-CE-1133), and the European Union's Horizon Europe
695 Research and Innovation programme under HORIZON-CL5-2022-D1-02 (grant no.

101081430-PARIS).

References

Aghedo, A. M., Bowman, K. W., Worden, H. M., Kulawik, S. S., Shindell, D. T., Lamarque, J. F., Faluvegi, G., Parrington, M., Jones, D. B. A., and Rast, S.: The vertical distribution of ozone instantaneous radiative forcing from satellite and chemistry climate models, Journal of Geophysical Research Atmospheres, 116, https://doi.org/10.1029/2010JD014243, 2011.

Anenberg, S. C., West, J. J., Fiore, A. M., Jaffe, D. A., Prather, M. J., Bergmann, D., Cuvelier, K., Dentener, F. J., Duncan, B. N., Gauss, M., Hess, P., Jonson, J. E., Lupu, A., Mackenzie, I. A., Marmer, E., Park, R. J., Sanderson, M. G., Schultz, M., Shindell, D. T., Szopa, S., Vivanco, M. G., Wild, O., and Zeng, G.: Intercontinental impacts of ozone pollution on human mortality, Environ Sci Technol, 43, 6482–6487, https://doi.org/10.1021/es900518z, 2009.

Ansari, T., Nalam, A., Lupaşcu, A., Hinz, C., Grasse, S., & Butler, T.: Explaining trends and changing seasonal cycles of surface ozone in North America and Europe over the 2000–2018 period: a global modelling study with NOx and VOC tagging, Atmospheric Chemistry and Physics, 25, 16833–16833. https://doi.org/10.5194/acp-25-16833-2025,2025.

Archibald, A. T., Neu, J. L., Elshorbany, Y. F., Cooper, O. R., Young, P. J., Frost, G. J., Galbally, I. E., Gerosa, G., Granier, C., and Griffiths, P. T.: Tropospheric Ozone Assessment Report : A critical review of changes in the tropospheric ozone burden and budget from 1850 to 2100, 1– 53, 2020.

Ashmore, M. R.: Assessing the future global impacts of ozone on vegetation, Plant Cell Environ, 28, 949–964, https://doi.org/10.1111/j.1365-3040.2005.01341.x, 2005.

719 Atkinson-Palombo, C. M., Miller, J. A., and Balling, R. C.: Quantifying the ozone “weekend
720 effect” at various locations in Phoenix, Arizona, Atmos Environ, 40, 7644–7658,
721 https://doi.org/10.1016/j.atmosenv.2006.05.023, 2006.

722 Auvray, M. and Bey, I.: Long-range transport to Europe: Seasonal variations and implications
723 for the European ozone budget, https://doi.org/10.1029/2004JD005503, 16 June 2005.

724 Bessagnet, B., Pirovano, G., Mircea, M., Cuvelier, C., Aulinger, A., Calori, G., Ciarelli, G.,

725 Manders, A., Stern, R., Tsyro, S., Garciá Vivanco, M., Thunis, P., Pay, M. T., Colette, A.,
726 Couvidat, F., Meleux, F., Rouïl, L., Ung, A., Aksoyoglu, S., Baldasano, J. M., Bieser, J.,
727 Briganti, G., Cappelletti, A., D’Isidoro, M., Finardi, S., Kranenburg, R., Silibello, C.,

728 Carnevale, C., Aas, W., Dupont, J. C., Fagerli, H., Gonzalez, L., Menut, L., Prévôt, A. S. H.,
729 Roberts, P., and White, L.: Presentation of the EURODELTA III intercomparison
730 exerciseevaluation of the chemistry transport models’ performance on criteria pollutants and
731 joint analysis with meteorology, Atmos Chem Phys, 16, 12667–12701,
732 https://doi.org/10.5194/acp-16-12667-2016, 2016.

733 Bonaccorso, B., Peres, D. J., Cancelliere, A., and Di Mauro, G.: Probabilistic forecasting of
734 drought class transitions in Sicily (Italy) using Standardized Precipitation Index and North
735 Atlantic Oscillation Index, Hydrol. Earth Syst. Sci., 19, 389–404, 2015.

736 Boylan, P., Helmig, D., and Oltmans, S.: Ozone in the Atlantic Ocean marine boundary layer,
737 1–13, https://doi.org/10.12952/journal.elementa.000045, 2014.

738 Butchart, N., Charlton-Perez, A. J., Cionni, I., Hardiman, S. C., Haynes, P. H., Krüger, K.,
739 Kushner, P. J., Newman, P. A., Osprey, S. M., Perlwitz, J., Sigmond, M., Wang, L., Akiyoshi,
740 H., Austin, J., Bekki, S., Baumgaertner, A., Braesicke, P., Brhl, C., Chipperfield, M.,
741 Dameris, M., Dhomse, S., Eyring, V., Garcia, R., Garny, H., Jöckel, P., Lamarque, J. F.,

742 Marchand, M., Michou, M., Morgenstern, O., Nakamura, T., Pawson, S., Plummer, D., Pyle,
743 J., Rozanov, E., Scinocca, J., Shepherd, T. G., Shibata, K., Smale, D., Teyssèdre, H., Tian,
744 W., Waugh, D., and Yamashita, Y.: Multimodel climate and variability of the stratosphere,
745 Journal of Geophysical Research Atmospheres, 116, https://doi.org/10.1029/2010JD014995,
746 2011.

747 Butler, T., Lupascu, A., Coates, J., and Zhu, S.: TOAST 1.0: Tropospheric ozone attribution
748 of sources with tagging for CESM 1.2.2, Geosci Model Dev,
749 11, 2825–2840, https://doi.org/10.5194/gmd-11-2825-2018, 2018.

750 Butler, T., Lupascu, A., and Nalam, A.: Attribution of ground-level ozone to anthropogenic
751 and natural sources of nitrogen oxides and reactive carbon in a global chemical transport
752 model, Atmos Chem Phys, 20, 10707–10731, https://doi.org/10.5194/acp-20-10707-2020,
753 2020.

754 Carslaw, D. C.: On the changing seasonal cycles and trends of ozone at Mace Head, Ireland,
755 Atmos. Chem. Phys, 3441–3450 pp., 2005.

756 Chang, K.-L., Schultz, M. G., Koren, G., & Selke, N.: Guidance note on best statistical 1108
757 practices for TOAR analyses. arXiv preprint arXiv:2304.14236, 2023.

758 Coates, J., Mar, K. A., Ojha, N., & Butler, T. M.: The influence of temperature on ozone
759 production under varying NO x conditions–a modelling study. Atmospheric Chemistry and
760 Physics, 16(18), 11601-11615, 2016.

761 Coleman, L., McVeigh, P., Berresheim, H., Martino, M., and O'Dowd, C. D.: Photochemical
762 impact on ozone fluxes in coastal waters, Advances in Meteorology, 2012,
763 https://doi.org/10.1155/2012/943785, 2012.

764 Coleman, L., Martin, D., Varghese, S., Jennings, S. G., and O'Dowd, C. D.: Assessment of
765 changing meteorology and emissions on air quality using a regional climate model: Impact
766 on ozone, Atmos Environ, 69, 198–210, https://doi.org/10.1016/j.atmosenv.2012.11.048,
767 2013.

768 Creilson, J. K., Fishman, J., & Wozniak, A. E. Intercontinental transport of tropospheric
769 ozone: A study of its seasonal variability across the North Atlantic utilizing tropospheric
770 ozone residuals and its relationship to the North Atlantic Oscillation. Atmospheric Chemistry
771 and Physics, 3(6), 2053–2066. https://doi.org/10.5194/acp-3-2053-2003,2003.

772 Crippa, M., Guizzardi, D., Butler, T. M., Keating, T., Wu, R., Kaminski, J., Kiesewetter, G.,
773 Im, U., Bessagnet, B., Chabrillat, S., et al.: The HTAP_v3 emission mosaic: merging regional
774 and global monthly emissions (2000–2018) to support air quality modelling and policies, Earth
775 Syst. Sci. Data, 15, 2667–2696, 2023.

776 Crippa, M., Guizzardi, D., Pagani, F., Schiavina, M., Melchiorri, M., Pisoni, E., Graziosi, F.,
777 Muntean, M., Maes, J., Dijkstra, L., Van Damme, M., Clarisse, L., and Coheur, P.: Insights
778 into the spatial distribution of global, national, and subnational greenhouse gas emissions in
779 the Emissions Database for Global Atmospheric Research (EDGAR v8.0), Earth Syst Sci
780 Data, 16, 2811–2830, https://doi.org/10.5194/essd-16-2811-2024, 2024.

781 Derwent, R. G.: Observation and interpretation of the seasonal cycles in the surface
782 concentrations of ozone and carbon monoxide at Mace Head, Ireland from 1990 to 1994,
783 Atmos Environ, 32, 2310, https://doi.org/10.1016/S1352-2310(97)00338-5, 1998.

784 Derwent, R. G., Simmonds, P. G., and Collins, W. J.: Ozone and carbon monoxide
785 measurements at a remote maritime location, mace head, Ireland, from 1990 to 1992, Atmos
786 Environ, 28, 2623–2637, https://doi.org/10.1016/1352-2310(94)90436-7, 1994.

Derwent, R. G., Collins, W. J., Johnson, C. E., and Stevenson, D. S.: Transient behaviour of tropospheric ozone precursors in a global 3-d ctm and their indirect greenhouse effects, 2001.

Derwent, R. G., Stevenson, D. S., Collins, W. J., and Johnson, C. E.: Intercontinental transport and the origins of the ozone observed at surface sites in Europe, Atmos Environ, 38, 1891– 1901, https://doi.org/10.1016/j.atmosenv.2004.01.008, 2004.

Derwent, R. G., Stevenson, D. S., Doherty, R. M., Collins, W. J., and Sanderson, M. G.: How is surface ozone in Europe linked to Asian and North American NOx emissions?, Atmos Environ, 42, 7412–7422, https://doi.org/10.1016/j.atmosenv.2008.06.037, 2008.

Derwent, R. G., Manning, A. J., Simmonds, P. G., Spain, T. G., and O'Doherty, S.: Analysis and interpretation of 25 years of ozone observations at the Mace Head Atmospheric Research Station on the Atlantic Ocean coast of Ireland from 1987 to 2012, Atmos Environ, 80, 361–368, https://doi.org/10.1016/j.atmosenv.2013.08.003, 2013.

Derwent, R. G., Manning, A. J., Simmonds, P. G., and Doherty, S. O.: Long-term trends in ozone in baseline and European regionally-polluted air at Mace Head, Ireland over a 30-year period, Atmos Environ, 179, 279–287, https://doi.org/10.1016/j.atmosenv.2018.02.024, 2018.

Derwent, R. G., Parrish, D. D., Manning, A. J., Spain, T. G., Simmonds, P. G., and O'Doherty, S.: Ozone at Mace Head, Ireland from 1987 to 2021: Declining baselines, phase-out of European regional pollution, COVID-19 impacts, Atmos Environ, 320, https://doi.org/10.1016/j.atmosenv.2023.120322, 2024.

Ding, J., Dai, Q., Fan, W., Lu, M., Zhang, Y., Han, S., and Feng, Y.: Impacts of meteorology and precursor emission change on O3 variation in Tianjin, China from 2015 to 2021, J Environ Sci (China), 126, 506–516, https://doi.org/10.1016/j.jes.2022.03.010, 2023.

Donlon, B., Cahalane, A., and Fanning, A.: Ireland's State of the Environment Report 2024 Editors, 2024.

Draxler, R. R. Evaluation of an Ensemble Dispersion Calculation. http://wesley.wwb.noaa.gov/reanalysis.html,2003.

EEA: Exceedance of air quality standards in Europe (Indicator AIR003, Issue.1109)2024 https://www.eea.europa.eu/en/analysis/indicators/exceedance-of-air-quality-standards

Emmons, L. K., Hess, P. G., Lamarque, J.-F., and Pfister, G. G.: Tagged ozone mechanism for MOZART-4, CAM-chem and other chemical transport models, Atmos. Chem. Phys., **12**, 4607–4622, https://doi.org/10.5194/acp-12-4607-2012,2012.

Finch, D. P., & Palmer, P. I., Increasing ambient surface ozone levels over the UK accompanied by fewer extreme events. Atmospheric Environment, 237, 117627, https://doi.org/https://doi.org/10.1016/j.atmosenv.2020.117627, 2020.

Fiore, A. M., Dentener, F. J., Wild, O., Cuvelier, C., Schultz, M. G., Hess, P., Textor, C., Schulz, M., Doherty, R. M., Horowitz, L. W., MacKenzie, I. A., Sanderson, M. G., Shindell, D. T., Stevenson, D. S., Szopa, S., Van Dingenen, R., Zeng, G., Atherton, C., Bergmann, D., Bey, I., Carmichael, G., Collins, W. J., Duncan, B. N., Faluvegi, G., Folberth, G., Gauss, M., Gong, S., Hauglustaine, D., Holloway, T., Isaksen, I. S. A., Jacob, D. J., Jonson, J. E., Kaminski, J. W., Keating, T. J., Lupu, A., Manner, E., Montanaro, V., Park, R. J., Pitari, G., Pringle, K. J., Pyle, J. A., Schroeder, S., Vivanco, M. G., Wind, P., Wojcik, G., Wu, S., and Zuber, A.: Multimodel estimates of intercontinental source-receptor relationships for ozone pollution, Journal of Geophysical Research Atmospheres, 114, https://doi.org/10.1029/2008JD010816, 2009.

832 Fowler, D., Coyle, M., Skiba, U., Sutton, M. A., Cape, J. N., Reis, S., Sheppard, L. J., Jenkins,
833 A., Grizzetti, B., Galloway, J. N., Vitousek, P., Leach, A., Bouwman, A. F., Butterbach-Bahl,
834 K., Dentener, F., Stevenson, D., Amann, M., and Voss, M.: The global nitrogen cycle in
835 theTwentyfirst century, Philosophical Transactions of the Royal Society B: Biological
836 Sciences, 368, https://doi.org/10.1098/rstb.2013.0164, 2013.

837 Girach, I. A., Tripathi, N., Nair, P. R., Sahu, L. K., and Ojha, N.: O3 and CO in the South
838 Asian outflow over the Bay of Bengal: Impact of monsoonal dynamics and chemistry, Atmos
839 Environ, 233, https://doi.org/10.1016/j.atmosenv.2020.117610, 2020.

840 Griffiths, P. T., Murray, L. T., Zeng, G., Shin, Y. M., Abraham, N. L., Archibald, A. T., Deushi,
841 M., Emmons, L. K., Galbally, I. E., Hassler, B., Horowitz, L. W., Keeble, J., Liu, J., Moeini,
842 O., Naik, V., and Connor, F. M. O.: Tropospheric ozone in CMIP6 simulations, 4187–4218,
843 2021.

844 Grigas, T., Ovadnevaite, J., Ceburnis, D., Moran, E., McGovern, F. M., Jennings, S. G., and
845 O'Dowd, C.: Sophisticated Clean Air Strategies Required to Mitigate Against Particulate
846 Organic Pollution, Sci Rep, 7, https://doi.org/10.1038/srep44737, 2017.

847 Guerreiro, C. B. B., Foltescu, V., and de Leeuw, F.: Air quality status and trends in Europe,
848 Atmos Environ, 98, 376–384, https://doi.org/10.1016/j.atmosenv.2014.09.017, 2014.

849 Huang, M., Carmichael, G. R., Pierce, R. B., Jo, D. S., Park, R. J., Flemming, J., Emmons, L.
850 K., Bowman, K. W., Henze, D. K., Davila, Y., Sudo, K., Jonson, J. E., Lund, M. T., Janssens-
851 Maenhout, G., Dentener, F. J., Keating, T. J., & Saiz-Lopez, A. (2017). Impact of
852 intercontinental pollution transport on North American ozone air pollution: An HTAP phase 2
853 multi-model study. Atmospheric Chemistry and Physics, 17(9), 5721–5750.
854 https://doi.org/10.5194/acp-17-5721-2017

IPCC, Masson-Delmotte, V., Zhai, P., Chen, Y., Goldfarb, L., Gomis, M. I., Matthews, J. B. R., Berger, S., Huang, M., Yelekçi, O., Yu, R., Zhou, B., Lonnoy, E., Maycock, T. K., Waterfield, T., Leitzell, K., & Caud, N. Working Group I Contribution to the Sixth Assessment Report of the Intergovernmental Panel on Climate Change Edited by. www.ipcc.ch,2021.

Jeon, W. B., Lee, S. H., Lee, H., Park, C., Kim, D. H., and Park, S. Y.: A study on high ozone formation mechanism associated with change of NOx/VOCs ratio at a rural area in the Korean Peninsula, Atmos Environ, 89, 10–21, https://doi.org/10.1016/j.atmosenv.2014.02.005, 2014.

Jonson, J. E., Stohl, A., Fiore, A. M., Hess, P., Szopa, S., Wild, O., Zeng, G., Dentener, F. J., Lupu, A., Schultz, M. G., Duncan, B. N., Sudo, K., Wind, P., Schulz, M., Marmer, E., Cuvelier, C., Keating, T., Zuber, A., Valdebenito, A., Dorokhov, V., De Backer, H., Davies, J., Chen, G. H., Johnson, B., Tarasick, D. W., Stübi, R., Newchurch, M. J., Von Der Gathen, P., Steinbrecht, W., and Claude, H.: A multi-model analysis of vertical ozone profiles, Atmos Chem Phys, 10, 5759–5783, https://doi.org/10.5194/acp-10-5759-2010, 2010.

Khiem, M., Ooka, R., Huang, H., Hayami, H., Yoshikado, H., and Kawamoto, Y.: Analysis of the Relationship between Changes in Meteorological Conditions and the Variation in Summer Ozone Levels over the Central Kanto Area, Advances in Meteorology, 2010, 1–13, https://doi.org/10.1155/2010/349248, 2010.

Lamarque, J. F. and Solomon, S.: Impact of changes in climate and halocarbons on recent lower stratosphere ozone and temperature trends, J Clim, 23, 2599–2611, https://doi.org/10.1175/2010JCLI3179.1, 2010.

878 Lamarque, J. F., Kinnison, D. E., Hess, P. G., and Vitt, F. M.: Simulated lower stratospheric
879 trends between 1970 and 2005: Identifying the role of climate and composition changes,
880 Journal of Geophysical Research Atmospheres, 113, https://doi.org/10.1029/2007JD009277,
881 2008.

882 Lamarque, J. F., Bond, T. C., Eyring, V., Granier, C., Heil, A., Klimont, Z., Lee, D., Liousse,
883 C., Mieville, A., Owen, B., Schultz, M. G., Shindell, D., Smith, S. J., Stehfest, E., Van
884 Aardenne, J., Cooper, O. R., Kainuma, M., Mahowald, N., McConnell, J. R., Naik, V., Riahi,
885 K., and Van Vuuren, D. P.: Historical (1850-2000) gridded anthropogenic and biomass
886 burning emissions of reactive gases and aerosols: Methodology and application, Atmos
887 Chem Phys, 10, 7017–7039, https://doi.org/10.5194/acp-10-7017-2010, 2010.

888 Lamarque, J. F., Emmons, L. K., Hess, P. G., Kinnison, D. E., Tilmes, S., Vitt, F., Heald, C.
889 L., Holland, E. A., Lauritzen, P. H., Neu, J., Orlando, J. J., Rasch, P. J., and Tyndall, G. K.:
890 CAMchem: Description and evaluation of interactive atmospheric chemistry in the
891 Community Earth System Model, Geosci Model Dev, 5, 369–411,
892 https://doi.org/10.5194/gmd-5-369-2012, 2012.

893

894 Lefohn, A. S., Malley, C. S., Smith, L., Wells, B., Hazucha, M., Simon, H., Naik, V., Mills,
895 G., Schultz, M. G., Paoletti, E., De Marco, A., Xu, X., Zhang, L., Wang, T., Neufeld, H. S.,
896 Musselman, R. C., Tarasick, D., Brauer, M., Feng, Z., Tang, H., Kobayashi, K., Sicard, P.,
897 Solberg, S., and Gerosa, G.: Tropospheric ozone assessment report: Global ozone metrics for
898 climate change, human health, and crop/ecosystem research,
899 Elementa, 6, https://doi.org/10.1525/elementa.279, 2018.

900 Lin, M., Fiore, A. M., Cooper, O. R., Horowitz, L. W., Langford, A. O., Levy, H., Johnson,
901 B. J., Naik, V., Oltmans, S. J., and Senff, C. J.: Springtime high surface ozone events over

902 the western United States: Quantifying the role of stratospheric intrusions, Journal of
903 Geophysical Research Atmospheres, 117, https://doi.org/10.1029/2012JD018151, 2012.

904 Lin, Y., Jiang, F., Zhao, J., Zhu, G., He, X., Ma, X., Li, S., Sabel, C. E., and Wang, H.: Impacts
905 of O_3 on premature mortality and crop yield loss across China, Atmos. Environ., **194**, 41–47,
906 https://doi.org/10.1016/j.atmosenv.2018.09.024, 2018.

907 Lupaşcu, A., Otero, N., Minkos, A., and Butler, T.: Attribution of surface ozone to NOx and
908 volatile organic compound sources during two different high ozone events, Atmos Chem
909 Phys, 22, 11675–11699, https://doi.org/10.5194/acp-22-11675-2022, 2022.

910 McVeigh, P., O'Dowd, C., and Berresheim, H.: Eddy Correlation Measurements of Ozone
911 Fluxes over Coastal Waters West of Ireland, Advances in Meteorology, 2010,
912 https://doi.org/10.1155/2010/754941, 2010.

913 Moiseenko, K. B., Vasileva, A. V., Skorokhod, A. I., Belikov, I. B., Repin, A. Y., and
914 Shtabkin, Y. A.: Regional Impact of Ozone Precursor Emissions on NOX and O3 Levels at
915 ZOTTO Tall Tower in Central Siberia, Earth and Space Science, 8,
916 https://doi.org/10.1029/2021EA001762, 2021.

917 Molod, A., Takacs, L., Suarez, M., and Bacmeister, J.: Development of the GEOS-5
918 atmospheric general circulation model: Evolution from MERRA to MERRA2, Geosci Model
919 Dev, 8, 1339–1356, https://doi.org/10.5194/gmd-8-1339-2015, 2015.

920 Monks, P. S., Archibald, A. T., Colette, A., Cooper, O., Coyle, M., Derwent, R., Fowler, D.,
921 Granier, C., Law, K. S., Mills, G. E., Stevenson, D. S., Tarasova, O., Thouret, V., Von
922 Schneidemesser, E., Sommariva, R., Wild, O., and Williams, M. L.: Tropospheric ozone and
923 its precursors from the urban to the global scale from air quality to short-lived climate forcer,
924 https://doi.org/10.5194/acp-15-8889-2015, 13 August 2015.

Nalam, A., Lupaşcu, A., Ansari, T., and Butler, T.: Regional and sectoral contributions of NO_x and reactive carbon emission sources to global trends in tropospheric ozone during the 2000–2018 period, Atmos. Chem. Phys., 25, 5287–5311, https://doi.org/10.5194/acp-25-5287-2025, 2025.

Nelson, B. S., et al.: Urban ozone trends in Europe and the USA (2000–2021), Atmos. Chem. Phys., 25, 16009–16032, https://doi.org/10.5194/acp-25-16009-2025, 2025

O'Dowd, C., Ceburnis, D., Ovadnevaite, J., Vaishya, A., Rinaldi, M., and Facchini, M. C.: Do anthropogenic, continental or coastal aerosol sources impact on a marine aerosol signature at Mace Head?, Atmos Chem Phys, 14, 10687–10704, https://doi.org/10.5194/acp-14-106872014, 2014.

Oltmans, S.J., Lefohn, A.S., Harris, J.M., Galbally, I., Scheel, H.E., Bodeker, G., Brunke, E., Claude, H., Tarasick, D., Johnson, B.J. and Simmonds, P.: Long-term changes in tropospheric ozone. Atmos Environ, 40(17), 3156-3173, https://doi.org/10.1016/j.atmosenv.2006.01.029. , 2006.

Oltmans, S. J., Lefohn, A. S., Shadwick, D., Harris, J. M., Scheel, H. E., Galbally, I., Tarasick, D. W., Johnson, B. J., Brunke, E. G., Claude, H., Zeng, G., Nichol, S., Schmidlin, F., Davies, J., Cuevas, E., Redondas, A., Naoe, H., Nakano, T., and Kawasato, T.: Recent tropospheric ozone changes - A pattern dominated by slow or no growth, Atmos Environ, 67, 331–351, https://doi.org/10.1016/j.atmosenv.2012.10.057, 2013.

Ordóñez, C., Garrido-Perez, J. M., & García-Herrera, R. Early spring near-surface ozone in Europe during the COVID-19 shutdown: Meteorological effects outweigh emission changes. Science of The Total Environment, 747, 141322. https://doi.org/https://doi.org/10.1016/j.scitotenv.2020.141322, 2020.

948 Pallé, E., and Butler, C.J.. :Comparison of sunshine records and synoptic cloud observations:
949 a case study for Ireland." Physics and Chemistry of the Earth, Parts A/B/C 27.6-8: 405-414,
950 2002.

951 Pan, C., Zhu, B., Gao, J., Hou, X., Kang, H., and Wang, D.: Quantifying Arctic lower
952 stratospheric ozone sources in winter and spring, Sci Rep, 8,
953 https://doi.org/10.1038/s41598018-27045-5, 2018.

954 Paoletti, E.: Impact of ozone on Mediterranean forests: A review, Environmental Pollution,
955 144, 463–474, https://doi.org/10.1016/j.envpol.2005.12.051, 2006.

956 Pausata, F. S. R., Pozzoli, L., Vignati, E., & Dentener, F. J.. North Atlantic Oscillation and
957 tropospheric ozone variability in Europe: Model analysis and measurements
958 intercomparison. Atmospheric Chemistry and Physics, 12(14), 6357–6376.
959 https://doi.org/10.5194/acp-126357-2012,2012.

960 Pio, C. A., Feliciano, M. S., Vermeulen, A. T., and Sousa, E. C.: Seasonal variability of ozone
961 dry deposition under southern European climate conditions, in Portugal, Atmospheric
962 Environment, 195–205 pp., 2000.

963 Russo, M. R., Kerridge, B. J., Abraham, N. L., Keeble, J., Latter, B. G., Siddans, R., Weber,
964 J., Griffiths, P. T., Pyle, J. A., and Archibald, A. T.: Seasonal , interannual and decadal
965 variability of tropospheric ozone in the North Atlantic : comparison of UM-UKCA and
966 remote sensing observations for 2005 – 2018, 6169–6196, 2023.

967 Saiz-Lopez, A., Mahajan, A. S., Abbatt, J., Bobrowski, N., Brown, S. S., Burrows, J. P.,
968 Carpenter, L. J., Chipperfield, M. P., Cuevas, C. A., Fernandez, R., Hossaini, R., Kinnison,
969 D. E., Lamarque, J.-F., Finlayson-Pitts, B. J., Plane, J. M. C., Platt, U., Pratt, K., Ravishankara,
970 A. R., Salawitch, R. J., Saltzman, E. S., Simpson, W. R., Solomon, S., Thornton, J. A., & Wang,

971 T.: The influence of short-lived halogens on atmospheric chemistry and climate, Nature, 648,
972 289–299, https://doi.org/10.1038/s41586-025-09753-x, 2025.

973 Seinfeld, J. H. and Pandis, S. N.: Atmospheric Chemistry and Physics: From Air Pollution to
974 Climate Change, 3rd edn., Wiley, Hoboken, NJ, 2016.

975 Shindell, D. T., Chin, M., Dentener, F., Doherty, R. M., Faluvegi, G., Fiore, A. M., Hess, P.,
976 Koch, D. M., Mackenzie, I. A., Sanderson, M. G., Schultz, M. G., Schulz, M., Stevenson, D.
977 S., Teich, H., Textor, C., Wild, O., Bergmann, D. J., Bey, I., Bian, H., Cuvelier, C., Duncan,
978 B. N., Folberth, G., Horowitz, L. W., Jonson, J., Kaminski, J. W., Marmer, E., Park, R.,
979 Pringle, K. J., Schroeder, S., Szopa, S., Takemura, T., Zeng, G., Keating, T. J., and Zuber, A.:

980 Atmospheric Chemistry and Physics A multi-model assessment of pollution transport to the
981 Arctic, Atmos. Chem. Phys, 5353–5372 pp., 2008.

982 Sicard, P., Serra, R., and Rossello, P.: Spatiotemporal trends in ground-level ozone
983 concentrations and metrics in France over the time period 1999-2012, Environ Res, 149,
984 122– 144, https://doi.org/10.1016/j.envres.2016.05.014, 2016.

985 Simmonds, P. G., Derwent, R. G., Manning, A. L., and Spain, G.: Significant growth in
986 surface ozone at Mace Head, Ireland, 1987-2003, Atmos Environ,
987 38, 4769–4778, https://doi.org/10.1016/j.atmosenv.2004.04.036, 2004.

988 Soares, J., Plass, D., Kienzler, S., González Ortiz, A., Gsella, A., Horálek, J. (2023). Health
989 Risk Assessment of Air Pollution: assessing the environmental burden of disease in Europe
990 in 2021 (Eionet Report – ETC HE 2023/7). European Topic Centre on Human Health and
991 the Environment. https://www.eionet.europa.eu/etcs/all-etc-reports

992 Spohn, T. K., Martin, D., Geever, M., and O'Dowd, C.: Effect of COVID-19 lockdown on
993 regional pollution in Ireland, Air Qual Atmos Health, 15,
994 221–234, https://doi.org/10.1007/s11869-021-01098-4, 2022.

995 Stein, A. F., Draxler, R. R., Rolph, G. D., Stunder, B. J. B., Cohen, M. D., and Ngan, F.: NOAA's
996 HYSPLIT atmospheric transport and dispersion modeling system, Bulletin of the American
997 Meteorological Society, 96, 2059–2077, https://doi.org/10.1175/BAMS-D-14-00110.1., 2015.

998 Stunder, B.J.B.: Global Data Assimilation System (GDAS) Archive Information, NOAA Air
999 Resources Laboratory, Silver Spring, MD, USA, December 1, 2004

1000 Sudo, K., and H. Akimoto, H.: Global source attribution of tropospheric ozone: Long-range
1001 transport from various source regions, J. Geophys. Res., 112, D12302,
1002 doi:10.1029/2006JD007992, 2007.

1003 Tan, J., Fu, J. S., Dentener, F., Sun, J., Emmons, L., Tilmes, S., Flemming, J., Takemura, T.,
1004 Bian, H., Zhu, Q., Yang, C. E., and Keating, T.: Source contributions to sulfur and nitrogen
1005 deposition - An HTAP II multi-model study on hemispheric transport, Atmos Chem Phys,
1006 18, 12223–12240, https://doi.org/10.5194/acp-18-12223-2018, 2018.

1007 Tavella, R. A. and da Silva Júnior, F. M. R.: Watch out for trends: did ozone increased or
1008 decreased during the COVID-19 pandemic?, Environmental Science and Pollution Research,
1009 28, 67880–67885, https://doi.org/10.1007/s11356-021-17142-w, 2021.

1010 Tilmes, S., Sanderson, B. M., and O'Neill, B. C.: Climate impacts of geoengineering in a
1011 delayed mitigation scenario, Geophys Res Lett, 43, 8222–
1012 8229, https://doi.org/10.1002/2016GL070122, 2016.

1013 Tilmes, S., Lamarque, J. F., Emmons, L. K., Kinnison, D. E., Ma, P. L., Liu, X., Ghan, S.,
1014 Bardeen, C., Arnold, S., Deeter, M., Vitt, F., Ryerson, T., Elkins, J. W., Moore, F., Spackman,

1015 J. R., and Val Martin, M.: Description and evaluation of tropospheric chemistry and aerosols
1016 in the Community Earth System Model (CESM1.2), Geosci Model Dev, 8, 1395–1426,
1017 https://doi.org/10.5194/gmd-8-1395-2015, 2015.

1018 Todorović, M. N., Radenković, M. B., Rajšić, S. F., & Ignjatović, L. M. Evaluation of
1019 mortality attributed to air pollution in the three most populated cities in Serbia. International
1020 Journal of Environmental Science and Technology, 16(11), 7059–7070.
1021 https://doi.org/10.1007/s13762019-02384-6, 2019.

1022 Tripathi, O. P., Jennings, S. G., O'Dowd, C. D., Coleman, L., Leinert, S., O'Leary, B., Moran,
1023 E., O'Doherty, S. J., and Spain, T. G.: Statistical analysis of eight surface ozone measurement
1024 series for various sites in Ireland, Journal of Geophysical Research Atmospheres, 115, 1–20,
1025 https://doi.org/10.1029/2010JD014040, 2010.

1026 Tripathi, O. P., Jennings, S. G., O'Dowd, C., O'Leary, B., Lambkin, K., Moran, E.,
1027 O'Doherty, S. J., and Gerard Spain, T.: An assessment of the surface ozone trend in Ireland
1028 relevant to air pollution and environmental protection, Atmos Pollut Res, 3,
1029 341–351, https://doi.org/10.5094/APR.2012.038, 2012.
1030 Tripathi, O. P., Jennings, S. G., Colman, L., Lambkin, K., Moran, E., and Dowd, C. O.: Ozone
1031 levels , changes and trends over Ireland – an Integrated Analysis, 2013.

1032 Vautard, R., Moran, M. D., Solazzo, E., Gilliam, R. C., Matthias, V., Bianconi, R., Chemel,
1033 C., Ferreira, J., Geyer, B., Hansen, A. B., Jericevic, A., Prank, M., Segers, A., Silver, J. D.,
1034 Werhahn, J., Wolke, R., Rao, S. T., and Galmarini, S.: Evaluation of the meteorological
1035 forcing used for the Air Quality Model Evaluation International Initiative (AQMEII) air
1036 quality simulations, Atmos Environ, 53, 15–37,
1037 https://doi.org/10.1016/j.atmosenv.2011.10.065, 2012

1038 Van Der Werf, G. R., Randerson, J. T., Giglio, L., Collatz, G. J., Mu, M., Kasibhatla, P. S.,
1039 Morton, D. C., Defries, R. S., Jin, Y., and Van Leeuwen, T. T.: Global fire emissions and the
1040 contribution of deforestation, savanna, forest, agricultural, and peat fires (1997-2009), Atmos
1041 Chem Phys, 10, 11707–11735, https://doi.org/10.5194/acp-10-11707-2010, 2010.

1042 Wespes, C., Hurtmans, D., Clerbaux, C., and Coheur, P. F.: O3 variability in the troposphere
1043 as observed by IASI over 2008-2016: Contribution of atmospheric chemistry and dynamics,
1044 J Geophys Res, 122, 2429–2451, https://doi.org/10.1002/2016JD025875, 2017.

1045 WHO: WHO global air quality guidelines: particulate matter (PM2.5 and PM10), ozone,
1046 nitrogen dioxide, sulfur dioxide and carbon monoxide, World Health Organization,
1047 https://iris.who.int/handle/10665/345329, 2021.

1048 Wild, O. & Ryan, E. M.: Quantifying and addressing the uncertainties in tropospheric ozone
1049 and OH in a global chemistry transport model, EGUsphere [preprint],
1050 https://doi.org/10.5194/egusphere-2025-4534, 2025.

1051 Yan, Y., et al.: Analysis of European ozone trends in the period 1995–2014, Atmos. Chem.
1052 Phys., 18, 5589–5605, https://doi.org/10.5194/acp-18-5589-2018, 2018.

1053 Yerramilli, A., Srinivas Challa, V., Rao Dodla, V. B., Myles, L. T., Pendergrass, W. R., Vogel,
1054 C. A., Tuluri, F., Baham, J. M., Hughes, R., Patrick, C., Young, J., & Swanier, S. Simulation
1055 of surface ozone pollution in the Central Gulf Coast region during summer synoptic condition
1056 using WRF/Chem air quality model. Atmospheric Pollution Research, 3(1), 55–71.
1057 https://doi.org/10.5094/APR.2012.005,2012.

1058 Young, P. J., Archibald, A. T., Bowman, K. W., Lamarque, J., Naik, V., Stevenson, D. S., and
1059 Tilmes, S.: Pre-industrial to end 21st century projections of tropospheric ozone from the
1060 Atmospheric Chemistry and Climate Model Intercomparison Project (ACCMIP), 2063–
1061 2090, https://doi.org/10.5194/acp-13-2063-2013, 2013.

Yu, H., Chin, M., West, J. J., Atherton, C. S., Bellouin, N., Bergmann, D., Bey, I., Bian, H., Diehl, T., Forberich, O., Hess, P., Schulz, M., Takemura, T., & Tan, Q.. A multimodel assessment of the influence of regional anthropogenic emission reductions on aerosol direct radiative forcing and the role of intercontinental transport. Journal of Geophysical Research: Atmospheres, 118(13), 7004–7025. https://doi.org/10.1002/jgrd.50502,2013.

Zhang, J. J., Wei, Y., & Fang, Z. Ozone pollution: A major health hazard worldwide. Frontiers in Immunology, 10(OCT), 1–10. https://doi.org/10.3389/fimmu.2019.02518,2019.

Zhang, C. and Stevenson, D.: Characteristic changes of ozone and its precursors in London during COVID-19 lockdown and the ozone surge reason analysis, Atmos. Environ., **273**, 118980, https://doi.org/10.1016/j.atmosenv.2022.118980,2022

Zhu, T., Melamed, M., Parrish, D., Gauss, M., Klenner, L. G.,Lawrence, M., Konare, A., and Liousse, C.: Impacts of Megaci-ties on Air Pollution and Climate, WMO, Geneva, 2012.

Figure Captions

Figure 1. The map of EPA O_3 measurement sites over Ireland with classification of backgrounds.

Figure 2. Annual average O_3 concentration at different sites in Ireland. In each box, the lowest whisker level represents the 5^{th} percentile, the box spans from the 25^{th} to the 75^{th}

1084 percentile, the horizontal line within the box represents the median 50th percentile, and the
1085 upper whisker represents the 95th percentile. The average of monthly O_3 values calculated
1086 for the entire period of each station, and the red line shows the average monthly O_3
1087 variation of all sites top axis shows the month (1– 12).

1088 **Figure 3**. Monthly trend analysis of O_3 at different sites for 10 year period. (2012-2022)
1089 Adopting the trend reliability scale defined for TOAR-II studies (Chang et al., 2023), trends
1090 with very high certainty are marked by ***($p \leq 0.001$), , trends with high certainty with
1091 **($p \leq 0.01$), and low to medium certainty with **($p \leq 0.05$). Positive trends are in red
1092 shade and negative trends are in blue shade.

1093 **Figure 5**.- Trend in O_3 precursors NO_2 (a), and CH_4 (b) at different sites. Trends with very
1094 high certainty are marked by ***($p \leq 0.001$), trends with high certainty with **($p \leq 0.01$),
1095 and low to medium certainty with *($p \leq 0.05$).

1096 **Figure 6**. Percentage change in NO_2 and O_3 during the lockdown period of 2020 as
1097 compared to the 2017-2019 average at different sites in Ireland for (a) March (b) April, (c)
1098 May Month.

1099 **Figure 7**. The comparison of Monthly CAM4 – Chem O_3 and Monthly O_3 observations at
1100 five sites in Ireland.

1101 **Figure 8**. Absolute contribution of major NO_x sources (a) (NO_x Tagging) and VOC source
1102 (b) (NOx Tagging) to the CAM4-Chem simulated surface O_3 for the Mace Head grid cell
1103 between 2000-2018.

1104 **Figure 9.** Trends in contributions to monthly average modelled Mace Head grid cell surface
1105 O_3 for the 2000-2018 period derived from (a) NO_x tagging and (b)VOC tagging.

1106 **Figure 10.** Trend in seasonal Average of observed O_3 (black) and Model O_3 (red) at Mace
1107 head, separated into clean sector and EU influenced sector.

Figure 11. Exceedances measured at Mace Head per month from 2000 until 2022, during the clean air sector(green) and EU influenced sector (yellow). The percentage of both to total exceedances is shown in the inlay.

Figure 12. (a) The trend in Spring-time exceedances measured at Mace Head between 2000 and 2022 (blue) with the clean-air exceedances (gold), and (b) The trend in the 95th percentile of spring (Mar- May) O_3 measured in µg /m^3 for the clean sector (blue) and the EU influenced sector (gold).

Figure 13 Monthly cumulative Mace Head grid cell O_3 contributions to EU influenced sector and clean sector exceedances (a) NO_x tagging and (b) VOC tagging Mace Head grid cell.